

ENVIRONMENTAL HISTORY OF ESTUARINE DISSOLVED OXYGEN INFERRED FROM  
TRACE-METAL GEOCHEMISTRY AND ORGANIC MATTER

by

GEOFFREY M. JOHNSON

A THESIS

Presented to the Department of Geography  
and the Graduate School of the University of Oregon  
in partial fulfillment of the requirements  
for the degree of  
Master of Science

December 2016

THESIS APPROVAL PAGE

Student: Geoffrey M. Johnson

Title: Environmental History of Estuarine Dissolved Oxygen Inferred from Trace-Metal Geochemistry

This thesis has been accepted and approved in partial fulfillment of the requirements for the Master of Science degree in the Department of Geography by:

Daniel G. Gavin                      Chairperson

Patricia McDowell                Member

and

Scott L. Pratt                      Dean of the Graduate School

Original approval signatures are on file with the University of Oregon Graduate School.

Degree awarded December 2016

© 2016 Geoffrey M. Johnson

## THESIS ABSTRACT

Geoffrey M. Johnson

Master of Science

Department of Geography

December 2016

Title: Environmental History of Estuarine Dissolved Oxygen Inferred from Trace-Metal Geochemistry

Environmental history recorded in sediments can track estuarine water quality through the use of geochemical and biological proxies. I collected sediment cores from two locations in the Coos Bay Estuary, at South Slough and Haynes Inlet, spanning from ~1680 AD to the present. To address the historical water column oxygen in the estuary I measured geochemical proxies including organic matter, magnetic susceptibility, and redox-sensitive metals to calibrate against a detailed 15-year record of dissolved oxygen observations. High visual correlation of these proxies and recent water quality supports the interpretation of long-term water quality from sediment cores. Finally, I provide evidence that potential low water quality has increased at South Slough, while decreasing or staying stable at Haynes inlet over the last 300 years. This history was explained by changing land use (logging, splash dams) effects on erosion and organic matter and the role of the dredged channel.

## CURRICULUM VITAE

NAME OF AUTHOR: Geoffrey M. Johnson

### GRADUATE AND UNDERGRADUATE SCHOOLS ATTENDED:

University of Oregon, Eugene

### DEGREES AWARDED:

Master of Science, Geography, 2016, University of Oregon  
Bachelor of Science, Environmental Science, 2014, University of Oregon

### AREAS OF SPECIAL INTEREST:

Long-term environmental change  
Human-environment interactions  
Future earth

### PROFESSIONAL EXPERIENCE:

Tutor, UO Services for Student Athletes, 2013-2014

Ecological Home Construction Consultant and Craftsman, Eugene, OR, 2005-2011

### GRANTS, AWARDS, AND HONORS:

Summa Cum Laude, University of Oregon, 2014

Offered Phi Beta Kappa, University of Oregon, 2014

Mortar Board Junior Scholar, University of Oregon, 2012

## ACKNOWLEDGMENTS

First, I acknowledge Drs. Dave Sutherland, Josh Roering and Dan Gavin for putting the Coos Bay project together and giving me the opportunity to participate, and to the Oregon SeaGrant for providing funding for coring trips and analysis. Also, to Nathan Mathabane and the aforementioned for help with coring the South Slough sites. Also, thanks to Drs. Patricia McDowell and Erin Herring for valuable comments during the drafting of this manuscript. Many additional thanks to Federico Cernucci and John Dilles of the Volcanism and Igneous Petrology lab at Oregon State University for their generous support and assistance with portable x-ray fluorescence spectrometry (pXRF). Similarly, thanks to Dr. Anders Carlson and Marco Esters for their help with using the line-scan XRF and benchtop XRF at OSU's Marine Core Facility and University of Oregon's CAMCOR respectively. More thanks to Drs. Erin Herring and Christof Schworer for their help with pollen extraction and analysis not to mention consistent optimism.

To my family, who remind me daily what matters most.

## TABLE OF CONTENTS

Chapter	Page
I. INTRODUCTION .....	1
1.1 Background and Context.....	1
1.2 Sediment Records of Paleo-Hypoxia from Estuaries and Coasts .....	4
II. MATERIALS AND METHODS .....	7
2.1 Site Details .....	7
2.1.1 Geologic Setting.....	7
2.1.2 Estuarine Dynamics and Ecological Context .....	7
2.1.3 Coos Bay History and Human Impacts.....	8
2.2 Methods.....	9
2.2.1 Core Collection and Locations.....	9
2.2.2 Core Processing and Physical Characteristics .....	10
2.2.3 Chronology .....	11
2.2.4 Geochemical Analysis .....	11
2.2.5 Pollen Analysis .....	12
2.2.6 Comparison of DO Observations and Sedimentary Proxies.....	12



Chapter	Page
III. RESULTS .....	14
3.1 Stratigraphy and chronology.....	14
3.2 Geochemical analysis.....	20
3.3 Dissolved oxygen observations compared to trace-metal geochemistry .....	24
3.4 Pollen proxy of land use and cover change .....	27
IV. DISCUSSION.....	28
4.1 Interannual variability in DO and metal concentrations in estuary sediment .....	29
4.2 Decoupled processes in the main estuary and the South Slough .....	33
4.3 Long-term proxies of water quality and human landscape effects in PNW estuaries .....	36
4.4 Geochemical proxies from pre- to post-settlement.....	38
4.5 Climate, pollen and land use and cover change 1630-present.....	39
V. CONCLUSIONS.....	42
APPENDICES .....	44
APPENDIX A. POLLEN FIGURES AND TABLES .....	44
APPENDIX B. USACE DREDGING RECORDS.....	45
REFERENCES CITED.....	47

## LIST OF FIGURES

Figure	Page
1. Site map of the Coos Bay Estuary and its watershed.....	3
2. Core physical characteristics.....	15
3. Age-depth model from Bayesian simulation of sedimentation.....	19
4. Ti, Mn, Ni, Zn, and Cr in sediment cores from surface cores .....	22
5. Line-scan XRF: Ti, Al, Ni, and Zn .....	23
6. 30-minute water logger data .....	25
7. Relationship between Ti erosion proxy with selected trace-metal DO proxies.....	26
8. Comparison of the Ni/Ti DO proxy from two core sites and the measured DO at Valino Island with upwelling indices (as a measure of coastal anoxia), median summer discharge of the South Fork Coos River, and timber harvest (as a measure of landscape impacts on water quality). .....	33
9. Long-term synthesis of anthropogenic and climatic forcings alongside Ni/Ti from pXRF (SS and HI) and core-scanning XRF-measured Ni/Ti (HI).....	37

## LIST OF TABLES

Table	Page
1. Core site location details.....	9
2. $^{210}\text{Pb}$ and $^{226}\text{Ra}$ activity.....	17
3. Radiocarbon dates.....	18

# CHAPTER I

## INTRODUCTION

### 1.1 Background and Context

Periods of anoxia in Oregon's ecologically and economically important coastal estuaries may be the result of both terrestrial and oceanic factors. Land-use impacts, such as logging, conversion of uplands and hillslopes to plantations, and wastewater disposal, can decrease oxygen in river water by increasing sediment loads and biological oxygen demand (Brown and Power 2011). Alternately, wind-driven upwelling offshore brings nutrient rich, low dissolved oxygen (DO) water up from depth. Severe anoxia in the California Current System (CCS) is a recent phenomenon within recorded history (the last 50 years); since 2002 the CCS has experienced severe hypoxia seasonally or annually (Chan et al. 2008; Sutherland and O'Neill 2016). At its most intense, in 2006, anoxia resulting from wind-driven upwelling resulted in the absence of all fish and near-complete mortality of macroscopic benthic invertebrates as well as the proliferation of shallow-water chemo-heterotrophic microbial mats on the Oregon continental shelf (Chan et al. 2008).

The recent low-DO events on the continental shelf in the Pacific Northwest highlight the need to assess their historical precedents and understand their link with estuarine water quality (Brown and Power 2011, O'Neill 2014). However, the degree to which water quality in Oregon estuaries is coupled with ocean processes is unclear. The seasonality and the interrelationships of river discharge, estuary dimensions, and openness to the ocean may all be important controls of estuarine DO (Sutherland and O'Neill 2016). Sutherland and O'Neill (2016) suggest strong seasonal hydrographic controls on estuarine DO, in which extended periods of low river discharge during summer months' result in biological feedbacks and eutrophication, which

coincide with the strong upwelling season in the CCS (Brown and Power 2011). Therefore, on decadal to centennial time scales, longer-term climatic variability may also affect these drivers of water quality in estuaries (i.e., Barron and Bukry 2007).

The natural variability of DO in seasonal PNW estuaries is not well constrained. While oxygen content has been measured for decades in several places on the Oregon Coast, the longer history is unknown. Anecdotal or archival evidence from documented observations is necessarily limited in temporal scope, but an alternative approach is the reconstruction of past environments using paleoenvironmental records. Estuaries are depositional environments, and sedimentary sequences are an excellent source of information about past events and processes taking place in the estuary, its watershed, and the adjacent ocean (Brush 2009; Gooday et al. 2009). Yet, the application of paleoenvironmental techniques to estuarine systems is a relatively recent development (Cronin et al. 2005; Scheiderich et al. 2010; Brandenberger et al. 2011).

In this study, I extend a 16-year measurement history of dissolved oxygen using a set of sediment cores from the Coos Bay Estuary (CBE). I developed a chronology for each core using lead-210 ( $^{210}\text{Pb}$ ) and radiocarbon ( $^{14}\text{C}$ ) dating, analyzed geochemical proxies of water column and sediment-water-interface oxygen concentration, analyzed the pollen record, and compared these to historical records of land-use change in the watershed.

In this study, I specifically addressed 1) Whether water-column dissolved oxygen is recorded in the sediment of Coos Bay, 2) Whether sedimentary signals from local and regional land-use and cover change (LUCC) are correlated to core-derived DO history, and 3) If sedimentary records of DO and LUCC vary longitudinally in the CBE. To address these questions, I quantified the elemental fractions of redox-sensitive metals and indicators of eutrophication in two sediment cores and compared these records with observed DO records,

river discharge, Pacific Decadal Oscillation indices (PDO), off-shore upwelling indices, sedimentary signals of land-use and cover change (i.e., pollen) and historical records of pre- and post-settlement landscapes.

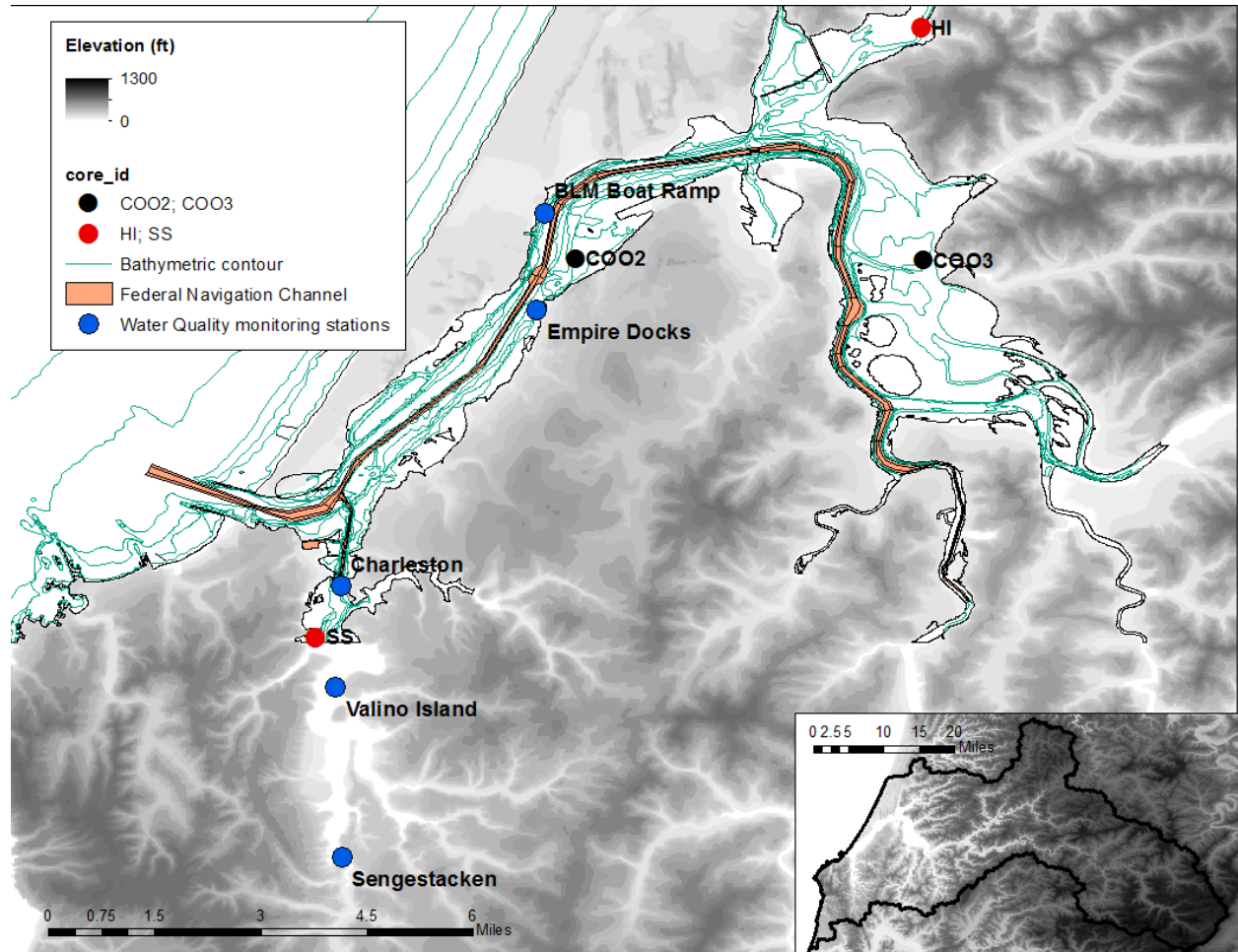


Figure 1. Site map of the Coos Bay Estuary and its watershed showing channel depth contours (10'), dredged channel, coring locations and water quality monitoring station in the CBE. The two analyzed cores, are SS (South Slough) and HI (Haynes Inlet); other unanalyzed sites are shown as black dots. Only DO observations from Valino Island were used in analysis. Data from NOAA, DOGAMI and SSNERR.

## **1.2 Sediment records of paleo-hypoxia from estuaries and coasts**

Geochemistry and mineralogy of sediment can be used to reconstruct water-quality conditions in the past. Many proxies have been developed to study water column DO in oceanic and lacustrine settings (Gooday et al. 2009). The diversity of techniques to reconstruct DO history is due to the broad-scale dependencies of biological communities in aquatic systems on DO and the importance of oxygen in biogeochemical processes that involve oxidation-reduction chemistry. The use of multiple complementary proxies is important for any environmental reconstruction. In dynamic coastal systems, the importance of multiple proxies is amplified by the complexity of climatic, oceanic and ecological mechanisms influencing DO proxies. In this regard, elemental indicators are valuable because individual elements have specific redox thresholds and thus provide the potential for discriminating low, middle and high concentrations of DO (Tribovillard et al. 2006, Gooday et al. 2009).

Several metal elements exhibit individual properties that provide a useful basis for reconstructing past redox conditions under a range of conditions (Tribovillard et al. 2006). Copper (Cu), nickel (Ni) and zinc (Zn) are typically delivered to the sediment-water interface associated with organic matter and are therefore good indicators of eutrophication. In contrast, cadmium (Cd), uranium (U), vanadium (V) and molybdenum (Mo) have redox chemistry that makes them sensitive to oxidation. Redox sensitive metals (RSM) may remobilize and will only precipitate from solution when threshold conditions permit (Gooday et al. 2009). Metals preserved in sediment represent the conditions at the sediment-water interface, which is generally the most oxygenated.

Organic matter is important for the preservation of trace metals in sediment both as a delivery vector and as a stabilization site if the supply of organic matter exceeds biotic demand.

When organic matter is consumed, complexed metals may be remobilized into the pore water and diffuse to the water column. Furthermore, organic matter preservation itself is a function of oxygen availability, burial rate and organic matter supply. In addition to organic matter, iron (Fe) and manganese (Mn) hydroxides and oxy-hydroxides stabilize trace metals by providing bonding sites. However, as with organic matter, post-depositional exposure to oxygen may alter mineral sites and further complicate interpretation. For these reasons, trace elements must be analyzed alongside organic matter and Fe and Mn. Context for weathering and transport of upland sediment is often provided through titanium (Ti) and aluminum (Al). Potassium (K) is similar to Al and typically should follow the same patterns. These elements do not undergo diagenetic transformation readily, thus they represent a reliable record of deposition. Normalizing other elemental proxies by either Ti or Al (or preferably both) of these metals allows us to determine enrichment rather than simply bulk concentration, which is useful under conditions where other metals (i.e. Ni, Zn) might be remobilized from the sediment upon oxidation of their complexes.

Elemental concentration data have become easier to obtain in recent years due to advances in x-ray fluorescence spectroscopy (XRF). Developments in energy dispersive XRF (EDXRF) and wave dispersive XRF (WDXRF) have dramatically reduced the costs as well as opening up opportunities for high-accuracy quantitative analysis (Weltje and Tjallingi 2008, Kenna et al. 2011). These advances make collection of large, diverse datasets, on elemental composition highly tractable for “big data” applications in paleoenvironmental science (e.g. Brewer et al. 2013). Novel analytical tools include EDXRF field portable systems (e.g. Kenna et al. 2011; Dahl et al. 2013) and whole-core scanning XRF (Weltje and Tjallingi 2008). Importantly, redox-sensitive trace elements (Fe and Mn) and eutrophication indicator elements



(Ni, Zn, Cu) in particular fall into the transition elements most precisely and accurately analyzed with these techniques.

Due to the relatively high DO status of the CBE and its sloughs, elemental proxies such as V, Cr, and Mo are not as useful for interpreting the history of water-column DO as they have been for ocean basins (Zheng et al. 2000; Dean et al. 2006) and deep, seasonally anoxic estuaries (Adelson et al. 2001; Scheiderich et al. 2010; Brandenberger et al. 2011). In the CBE, and other small seasonal PNW estuaries, nutrient loading from wastewater and agricultural activities (Brown and Power 2011), and organic matter loading from forest clearance and rafting timber (Sedell et al. 1991; Ringler and Hall 1975) have led to symptoms of eutrophication. Thus, these causes of low DO should be best represented in sediments from indicators of eutrophic potential (e.g. Zn and Ni), and their normalized ratios to erosion proxies (e.g. Al and Ti; Gooday et al. 2009).

## **CHAPTER II**

### **MATERIALS AND METHODS**

#### **2.1 Site details**

##### **2.1.1 Geologic setting**

The 5,383 ha Coos Bay estuary (CBE; 43.35 N, 124.33 W) in the Oregon Coast Range is composed of several large sloughs and inlets. The 157,645 ha watershed contains urban and agricultural areas and forested steep terrain reaching 600 m a.s.l. (Figure 1). The bedrock is primarily Eocene sandstones of the Tyee formation and other continental margin sediments. The highly maritime climate is marked by moderated winter (7-8 °C) and cool summer (14-16 °C) temperatures. Precipitation averages 1500 mm/yr, falling primarily as rain during October-April. Regional uplift due to the Cascadia Subduction Zone activity is muted locally by seismic subsidence (Kelsey et al. 1998). The most recent subsidence event in 1700 CE resulted in a 1 m vertical displacement in South Slough, CBE (Nelson et al. 1996), which likely created an equal amount of accommodation space for sediment infilling. Slower, background subsidence from crustal deformation, as well as sea level rise, are additional influences that could affect aggradation rate.

##### **2.1.2 Estuarine Dynamics and Ecological Context**

The CBE is near the southern end of the Pacific Northwest (PNW) coastal temperate rainforest. CBE is a seasonal estuary that is tidally dominated for most of the year due the greater influx of oceanic water during a tidal cycle than river discharge. Winter conditions are characterized by high precipitation leading to higher river discharge, higher water column stratification and migration of the salt-wedge intrusion toward the ocean (Sutherland and O'Neill

2016). During summer, lower precipitation leads to greater tidal influence and slower turnover of estuary water (Rumrill 2007; O'Neill 2014).

### **2.1.3 Coos Bay History and Human Impacts**

Coos Bay is the second largest estuary in Oregon and the deepest draft port, which has made it an economic hub of southern Oregon for the past century (Douthit 1997, Peterson 1972). The Port of Coos Bay requires dredging of mid-channel sediments multiple times per year from the mouth of the estuary to downtown Coos Bay, a distance of ~24km. Virtually all dredging activities occur from June to October. In-estuary filling with dredged material was common prior to 1970, however, the majority of dredge spoils are removed to the continental shelf since then (Appendix B: Figure 1, 2).

Prior to Euro-American settlement, early Americans populated the coast by at least 8500-8400 BP (<sup>14</sup>C calibrated years) and lived in relative stability with consistent increases in population and minor changes in their hunter-gatherer lifestyle (Erlandson et al. 2008). When European contact began in the 16<sup>th</sup> century, there were few changes to the social and economic structure of the local population until 1820-30 when smallpox and measles epidemics killed an estimated 70 percent of the inhabitants (Youst 1997). By 1850-60, however, the first Euro-American communities became established. Logging, mining, and agriculture began almost simultaneously, but have had dramatically different trajectories through time and space (Lansing 2005, 2007). Mining in particular was not widely successful in the CBE watershed. Small coal veins southwest of Coos Bay were quickly discovered, but none was productive after 1934 (Lansing 2005). Timber continues to be an important economic component of the whole South coast region, however harvests peaked between 1954 and 1965. Agriculture in Coos County also peaked mid-century at 28% of county's land area including woodlots, pasture and cropland in

1950. The area in farms has decreased by ~50% since 1950 (USDA 2016), and today is a relatively minor economic activity (Lansing 2005) consisting of hobby farms, hay production and small dairy enterprises.

## 2.2 Methods:

### 2.2.1 Core collection and locations

I collected surface cores using an 8-cm diameter polycarbonate tube fitted with a piston. Five cores were collected on March 18, 2014 (COO1-5, Figure 1, Table 1). A sixth site (COO6) was collected on Sept 10, 2015 using a combination of the surface corer and three 1 m overlapping drives with a Livingstone piston corer in order to reach greater depths. The two sites with the least disturbed sediments (assessed by preliminary  $^{210}\text{Pb}$  analysis) were selected for detailed studies: COO4 in South Slough (hereafter SS) and COO6 in Haynes Inlet (hereafter HI). The elevation of the mud-water interface at each core site relative to mean low-low water (MLLW) was estimated using a combination of water depth at the time of coring with respect to tidal corrections published by NOAA (data available at <http://tidesandcurrents.noaa.gov/>). According to this method, both sites are below MLLW (Table 1), although periodic exposure to the air may occur semiannually at South Slough.

Table 1. Core site location details in the Coos Bay estuary, Oregon. Elevation relative to MLLW was estimated using the tide level at Charleston, OR; the tidal peak offset at North Bend, OR (for HI only; see data supplement); and the water depth recorded at the time of coring

<b>Core site</b>	<b>Location</b>	<b>Core length (cm)</b>	<b>Water depth (cm above MLLW)</b>
South Slough (SS)	43° 19.545'N 124° 19.541'W	81	90
Haynes Inlet (HI)	43° 27.117'N 124° 12.110'W	180	215

### **2.2.2 Core processing, loss-on-ignition, and magnetic susceptibility**

The upper 10 cm of the SS core and the upper 14 cm of the HI surface core were extruded and subsampled into Whirlpak bags in the field upon returning to shore. The remainder of the SS core was immediately stored in a refrigerator and subsectioned in continuous 1-cm intervals in the laboratory within 2 days of collection. Each 1-cm interval sample was dried, ground lightly and picked free of visually identified pieces of organic detritus. The HI surface core was also subsectioned in continuous 1-cm intervals in the laboratory and refrigerated in plastic bags. Unlike at SS, I did not dry and grind 1-cm sections of the HI core, but rather subsampled for further analyses prior to each analysis. The three Livingstone drives were split longitudinally. One half was used as a “working core” to subsample for additional analyses, and the other was placed in a freezer to archive redox-sensitive geochemical properties and was used for core-scanning XRF.

I estimated organic matter content by loss-on-ignition (Heiri et al. 2001). For SS, each 1-cm section was analyzed. For HI, in the top 36 cm, LOI subsamples were spaced evenly at 1 cm intervals. Below 36 cm subsamples are located at the visual transitions of either color or texture, or every 5 cm, whichever was least. Lastly, I measured specific magnetic susceptibility (MS) of the SS surface core (1-cm subsamples) using a Sapphire Instruments magnetic susceptibility cup meter.

### 2.2.3 Chronology

For all 1-cm subsamples of the SS core,  $^{210}\text{Pb}$  activity was determined using a CANBERRA low-energy Germanium detector at 46.5 keV (Mathabane 2015). Dry mass between 25 and 70 g were used for this analysis. I used data from Mathabane (2015) to construct age and mass accumulation models for the upper 30 cm of the core using the constant rate of supply (CRS) model (Appleby and Oldfield 1978; Binford 1990). A single AMS radiocarbon ( $^{14}\text{C}$ ) date on identifiable conifer needles was obtained from the bottom of the SS core. For the HI core,  $^{210}\text{Pb}$  activity was measured on ten subsamples spaced from 2 to 80 cm by Flett Research Ltd using a polonium spike method modified from Eakins and Morrison (1978). In situ radium production was also quantified at 4 depths to approximate the background production of  $^{210}\text{Pb}$  (Mathieu et al. 1988). Radiocarbon dates were obtained from four depths in the HI core. In cases where identifiable conifer needles were not found, I used coarse ( $>250\ \mu\text{m}$ ) organic detrital material. Radiocarbon dates were calibrated using CALIB Rev 7.0.4 software (Stuiver and Reimer 1993) with the IntCal13 calibration curve (Reimer et al. 2013). I computed final age-depth models using Bacon 2.2 (Blaauw and Christen 2011), a Bayesian algorithm that iteratively simulates the sedimentation process to arrive at a set of chronologies given the uncertainties of the  $^{210}\text{Pb}$  and calibrated  $^{14}\text{C}$  chronological controls.

### 2.2.4 Geochemical analysis

For the surface cores at both sites, XRF analysis of dried, ground sediment on each 1-cm section was made using a Bruker Tracer IV Geo portable x-ray fluorescence spectrometer (pXRF) in soil mode. All pXRF measurements were taken at 40kEV and 25mA. From the HI site, the Livingstone cores were analyzed on an ITRAX core-scanning XRF at Oregon State University. For these analyses, I used the frozen archived cores thawed out temporarily. The

surface preparation needed was minimal due to the smoothness of the sediment and consisted of careful scraping with a knife perpendicular to the core axis.

### **2.2.5 Pollen analysis**

I carried out pollen analysis on dried, ground sediment from SS according to standard procedures in Faegri et al. (1989). Extracted pollen was mounted on slides in silicon oil and a minimum of 250 grains counted at 400x magnification. I identified pollen grains to the lowest possible taxonomic unit, and functional groups according to disturbance adaptation (Data supplement, Table 1) were applied to evaluate the trend in land-use and cover change. Processing subsamples for pollen required a minimum of 3 overnight hydrofluoric acid treatments due to high silica content. All pollen counts are shown as percentage of total pollen spectra.

### **2.2.6 Comparison of DO observations and sedimentary proxies**

30-minute DO observations from a moored water quality monitoring station at Valino Island in South Slough (Figure 1) have been continually recorded since 1999 (SSNERR 2016). The Charleston Bridge station has been operational since 2002, but is more indicative of conditions in the CBE main channel mouth than Valino Island. To assess the duration of low DO conditions, I added up the number of individual 30-minute records from the DO data during each calendar year for which the recorded DO was below geochemically relevant thresholds of 5, 4, 3, 2, and 1 mg/L. For all correlative analyses and visualizations, I used the 5 mg/L threshold, which is below the biologically impaired limit of 6.5 mg/L established by the Oregon Department of Environmental Quality (ODEQ). 5 mg/L has been used as a threshold for the preservation of redox sensitive geochemical indicators like V and Cr (Gooday et al. 2009). Other metals of interest (Ni, Zn, and Cu) should respond to DO levels insofar as the consumption of organic matter and remobilization of Fe and Mn oxyhydroxides are associated with oxygen availability.

Direct comparison of proxies and DO measurements using required the use of the age-depth modeling described above. Each 1 cm increment represented more than 1 year, so to account for the difference between the temporal resolution of DO and core-derived proxy data, I plotted the geochemical data on unequal time bins and overlaid the annual DO statistics described above. I plotted only DO comparisons for the SS core, because HI is too far from the monitoring stations operated by the SSNERR, which are the only stations in the CBE with long enough histories to make robust comparisons to core-derived proxies.



## CHAPTER III

### RESULTS

#### 3.1 Stratigraphy and Chronology

At SS, the 81-cm core consisted of interbedded oxidized, lighter (2.5 YR 3/0) sediment and darker, reduced (2.5 YR 3/2) silty sediment (Figure 2). Detailed color and texture information was not possible following extrusion of the SS core into plastic bags; however, CT scanning of the SS core carried out by Mathabane (2015) suggests a mixing window of up to 5cm. The proportion of organic matter, estimated by LOI, shows a rapid increase from ~5% to 21.9 % in the upper 30 cm of SS (Figure 2), before dropping to 6.7 % in the upper-most 4 cm. Specific magnetic susceptibility ( $\chi_m$ ) exhibits a similar pattern: below 30 cm lower values predominate, and above 30 cm  $\chi_m$  steadily increases to the top 1cm. In contrast to the LOI,  $\chi_m$  does not drop as substantially in the upper 4 cm.

The  $^{210}\text{Pb}$  profile declined exponentially from 12.1 dpm/g near the surface to a constant background level of 2.6 dpm/g at a depth of 28 cm (Table 2). The CRS-estimated ages from the  $^{210}\text{Pb}$  profile (0-31 cm) were linked to the radiocarbon age (80 cm) using the BACON age-depth model (Figure 3). There is a nearly linear age-depth relationship above 19 cm (ca. 1968 AD) with a sedimentation rate of 0.9 cm/yr. Below 19 cm, there is a distinctly lower sedimentation rate (0.51 cm/yr) to the bottom of the  $^{210}\text{Pb}$  profile. Between the lower-most  $^{210}\text{Pb}$  date (ca. 1864 AD) and the  $^{14}\text{C}$  date (ca. 1630 AD) the average sedimentation rate is 0.23 cm/yr. The standard deviation (SD) of age estimates for the upper 15 cm (1979-2014) ranges from 4.4 to 5.0 yr., whereas the SD of age estimates from 15 to 30 cm range from 5.1 to 37.4 yr.

At the HI site, 180 cm of sediment was recovered. The sediment was composed of interbedded lighter and darker sediment in the upper 90 cm with sand layers at 45 and 74 cm of 5

cm and 2 cm, respectively (Figure 2). Below 90 cm, similar light-dark interbedding is punctuated by frequent narrow sand layers and black (2.5 YR 2/0) and very light brown (10 YR 3/3) layers between 104 cm and 119 cm. LOI is low (<8%) throughout the core. The upper 40 cm of the HI core is characterized by lower variability in LOI (6-7%), whereas below 40 cm variation ranges from 4 to 8%.

Measured lead activity at HI was much lower than at SS with the highest total activity at 2.30 dps at 6 cm depth (Table 2). The  $^{210}\text{Pb}$  activity does not reach the supported background (as estimated from Ra-226 measurements) until between 60 and 80 cm depth. The combined  $^{210}\text{Pb}$  and  $^{14}\text{C}$  age model (Figure 3) for HI shows a similar pattern to SS, with higher sedimentation rates in the past 50 years, preceded by lower rates to the lower-most  $^{210}\text{Pb}$  date. In the gap between  $^{210}\text{Pb}$  and  $^{14}\text{C}$  long-term average sedimentation rates are lower than 0-50 ybp, and higher than 50-120 ybp.

Radiocarbon dates at HI at 100.5, 147, and 165 cm were wood fragments (Table 3). Of those, the upper two are older than the trend suggested by the  $^{210}\text{Pb}$  age model and are consistent with redeposited detrital material. In contrast, the HI date at 180 cm and the SS date at 81 cm were derived from fine detritus that likely have a short residence time prior to burial. Therefore, of the three dates deemed to be usable, two were from fine detritus and one was from a wood fragment, while two out of three wood fragments were most likely redeposited material and excluded from the age model.

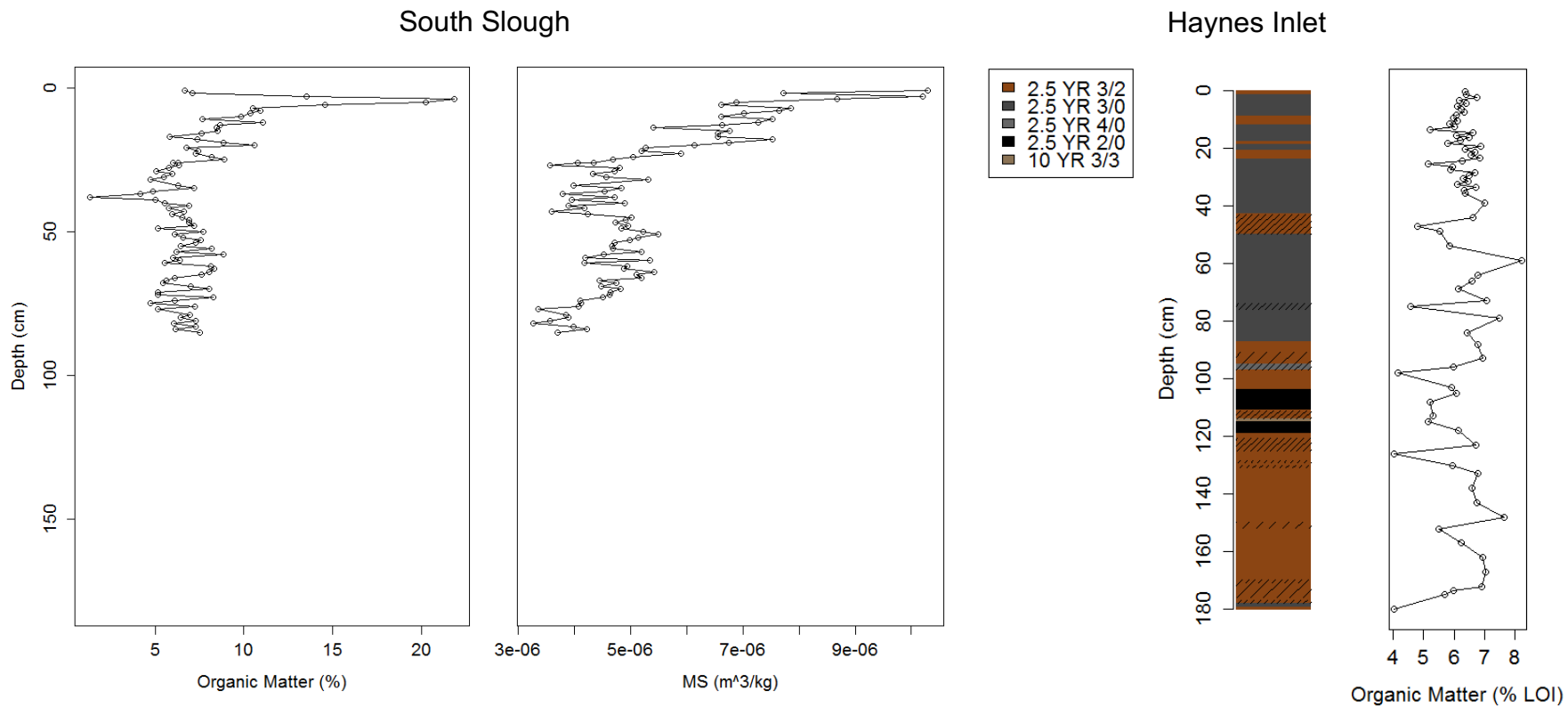


Figure 2. Physical core characteristics. Left two panels show the LOI and MS of the SS core. The right two panels show the stratigraphy of Munsell color and qualitative estimates of sand content from visual core examination and estimates of organic matter from LOI of the HI core. Qualitative estimates of moderate and high sand content are represented as cross-hatch density, although sand-sized clasts were present at every depth.

Table 2.  $^{210}\text{Pb}$  and  $^{226}\text{Ra}$  activity from sediments at two sites in CBE.  $^{210}\text{Pb}$  Measurements at SS were previously published by Mathabane (2015).  $^{210}\text{Pb}$  measurements at HI were made by Flett Research Ltd, Winnipeg. Ages were estimated by a constant-rate-of-sedimentation model following Binford (1990).

Depth (cm)	Activity (dpm/g)	Modelled Age (ybp)	Calendar Date A.D.
South Slough			
0 - 1	5.8 ± 2.4	1.3 ± 4.0	2013.0
1 - 2	6.3 ± 2.5	3.3 ± 4.1	2011.0
2 - 3	11.0 ± 3.3	5.3 ± 4.0	2008.9
3 - 4	12.1 ± 3.5	8.0 ± 4.0	2006.3
4 - 5	10.7 ± 3.2	10.5 ± 4.0	2003.8
5 - 6	9.4 ± 3.1	11.9 ± 4.0	2002.3
6 - 7	8.4 ± 2.9	14.0 ± 4.0	2000.3
7 - 8	7.8 ± 2.8	15.8 ± 4.0	1998.4
8 - 9	7.2 ± 2.7	17.9 ± 4.1	1996.4
9 - 10	6.7 ± 2.9	19.7 ± 4.1	1994.6
10 - 11	6.3 ± 2.5	22.1 ± 4.1	1992.2
11 - 12	5.9 ± 2.5	24.4 ± 4.2	1989.9
12 - 13	5.6 ± 2.4	27.3 ± 4.3	1987.0
13 - 14	5.3 ± 2.4	29.4 ± 4.2	1984.9
14 - 15	5.1 ± 2.4	32.4 ± 4.5	1981.9
15 - 16	4.8 ± 2.2	35.6 ± 4.6	1978.7
16 - 17	4.4 ± 2.1	38.7 ± 4.7	1975.5
17 - 18	4.7 ± 2.2	42.6 ± 4.9	1971.6
18 - 19	4.5 ± 2.2	46.3 ± 4.9	1967.9
19 - 20	4.3 ± 2.2	50.1 ± 5.1	1964.2
20 - 21	4.2 ± 2.2	55.0 ± 6.0	1959.2
21 - 22	4.0 ± 2.0	59.7 ± 5.8	1954.6
22 - 23	3.7 ± 2.0	65.3 ± 7.0	1949.0
23 - 24	3.5 ± 2.0	70.1 ± 7.0	1944.2
24 - 25	3.2 ± 2.0	75.4 ± 8.6	1938.8
25 - 26	2.9 ± 1.7	81.1 ± 9.4	1933.1
26 - 27	2.8 ± 1.7	87.9 ± 11.8	1926.4
27 - 28	2.7 ± 1.7	95.6 ± 14.4	1918.7
28 - 29	2.6 ± 1.6	104.9 ± 18.3	1909.4
29 - 30	2.7 ± 1.6	118.5 ± 26.1	1895.7
30 - 31	2.8 ± 1.7	149.7 ± 76.0	1864.6
Haynes Inlet			
$^{210}\text{Pb}$			
0 - 2	1.9 ± 0.2	1.2 ± 0.3	2014.6
4 - 6	2.3 ± 0.2	4.9 ± 0.3	2010.9
8 - 10	1.7 ± 0.1	8.4 ± 0.3	2007.4

14 - 15	1.5 ± 0.1	12.2 ± 0.3	2003.5
22 - 23	2.0 ± 0.1	21.2 ± 0.3	1994.6
30 - 31	1.4 ± 0.1	31.9 ± 0.3	1983.8
39 - 40	1.0 ± 0.1	42.3 ± 0.4	1973.5
44 - 45	1.2 ± 0.1	50.7 ± 0.4	1965.1
59 - 60	0.7 ± 0.1	85.7 ± 0.9	1930.0
79 - 80	0.5 ± 0.1	142.0 ± 4.6	1873.8
<sup>226</sup> Ra			
9 - 10	0.43 ± 0.03	-	-
39 - 40	0.36 ± 0.02	-	-
44 - 45	0.36 ± 0.02	-	-
59 - 60	0.49 ± 0.02	-	-
79 - 80	0.40 ± 0.02	-	-

Table 3. Radiocarbon dates from two sediment cores in the Coos Bay estuary.

CAMS #	Sample Depth (cm)	<sup>14</sup> C age	Dated Material
South Slough			
173967	80-81	335 ± 35	Fine detritus
Haynes Inlet			
173346	100.5*	295 ± 40	Wood
173969	147*	725 ± 30	Wood
173347	165	180 ± 30	Wood
173968	179-180	270 ± 35	Fine detritus

\* Date rejected due to age reversal; likely result of older wood fragments and/or redeposited material.

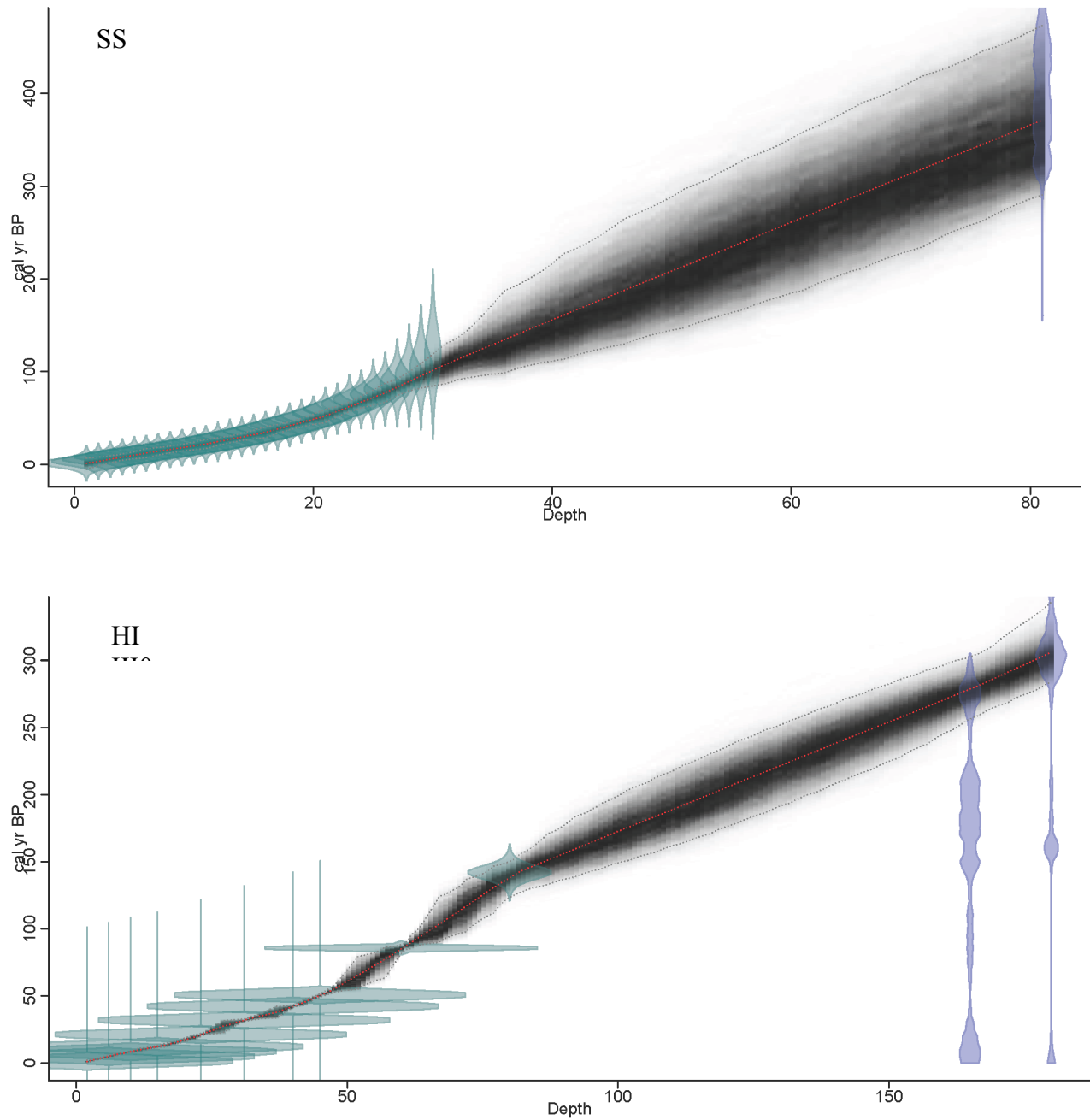


Figure 3. Age-depth model from Bayesian simulation of sedimentation in the R program Bacon (Blaauw and Christen 2011) for the South Slough (top) and Haynes Inlet (bottom). Each plot shows  $^{210}\text{Pb}$  age model estimates (in green polygons) and  $^{14}\text{C}$  dates (in purple). The red line is the mean of all iterations while the grey-scale shows the interpolated range of likely ages between dated subsections.

### 3.2 Geochemical analysis

At SS, bulk concentration of Mn increased above 40 cm, and most in the upper 20 cm (Figure 4). Ti also increased noticeably in the upper 15 cm, however the overall variability in Ti is marked by sections of low homogenous values at 15-20 cm and 40-53 cm occurring between sections marked by higher variability. A slight decrease in Ti is evident from 80 to 40 cm. Ni/Ti and Zn/Ti have high short-term variability in the upper 20 cm reflecting the influence of Ti, and like Ti the most pronounced effect is in the upper-most 15 cm. Both Ni/Ti and Zn/Ti show long-term average increase from above 40 cm similar to Mn. Below 40 cm, these two ratios show little trend. Cr, a redox-sensitive metal, does not behave in the same way and has little apparent relationship to other elements. While Cr does show a slight increase in the upper 20 cm, it is similar to the variability in the lower portion of the core (Figure 4). Several high Cr values occur below 50 cm. Other redox-sensitive metals (Cd, V, U, and Mo in particular) were not well resolved using the pXRF technique and detection limits of the instrument restrict further use of these elements. Other important geochemical indicators not shown in Figure 4 followed the same patterns as those shown here. Fe is very similar to Mn while Cu is similar to Ni and Zn. In addition to these macroscopic trends, there is finer scale variability in all proxies although systematic trends are not obvious.

At HI, the surface core corresponds to only the last ca. 50 years of sedimentation. Furthermore, selected metals (Mn, Zn and Ni), erosion indicators (Ti and Al) and erosion-normalized ratios show different patterns whether derived from the pXRF approach (on the surface core; Figure 4) or the high resolution core-scanning XRF (on the parallel Livingstone cores; Figure 5). The HI surface core (pXRF data) indicates a change in element concentrations between 15 and 20 cm with increased preservation of Mn at this depth. Mn shows a slight yet

consistent increasing trend from 50 to 20 cm. Ni/Ti, Zn/Ti and Cr/Ti ratios exhibit similar peaks to those for Mn but with additional small peaks at 23, 37, and 47 cm. In contrast to Mn, there is an overall reduction in Ni/Ti and Zn/Ti that is interrupted by a broad peak at 17 cm. For the core-scanning XRF, Al was included as an additional erosion indicator; Al was not available from the pXRF in soil-mode. Above 75 cm, Al counts are quite low on average, while large peaks are also present. Below 75 cm there is a higher average Al but with low variability. Ti peaks fall at the same depths as Al peaks, although peak shapes and intensity are highly variable and there is an anomalous section between 5 and 15 cm with high Ti and low Al counts. Much of the core is characterized by an inverse relationship between erosion indicators (Ti and Al) and indicator metals, which enhances the variability in the erosion-normalized ratios. Core-scanning Ni/Ti and Zn/Ti decline in the upper 80 cm, roughly corresponding to the last 100 years (Figure 5).



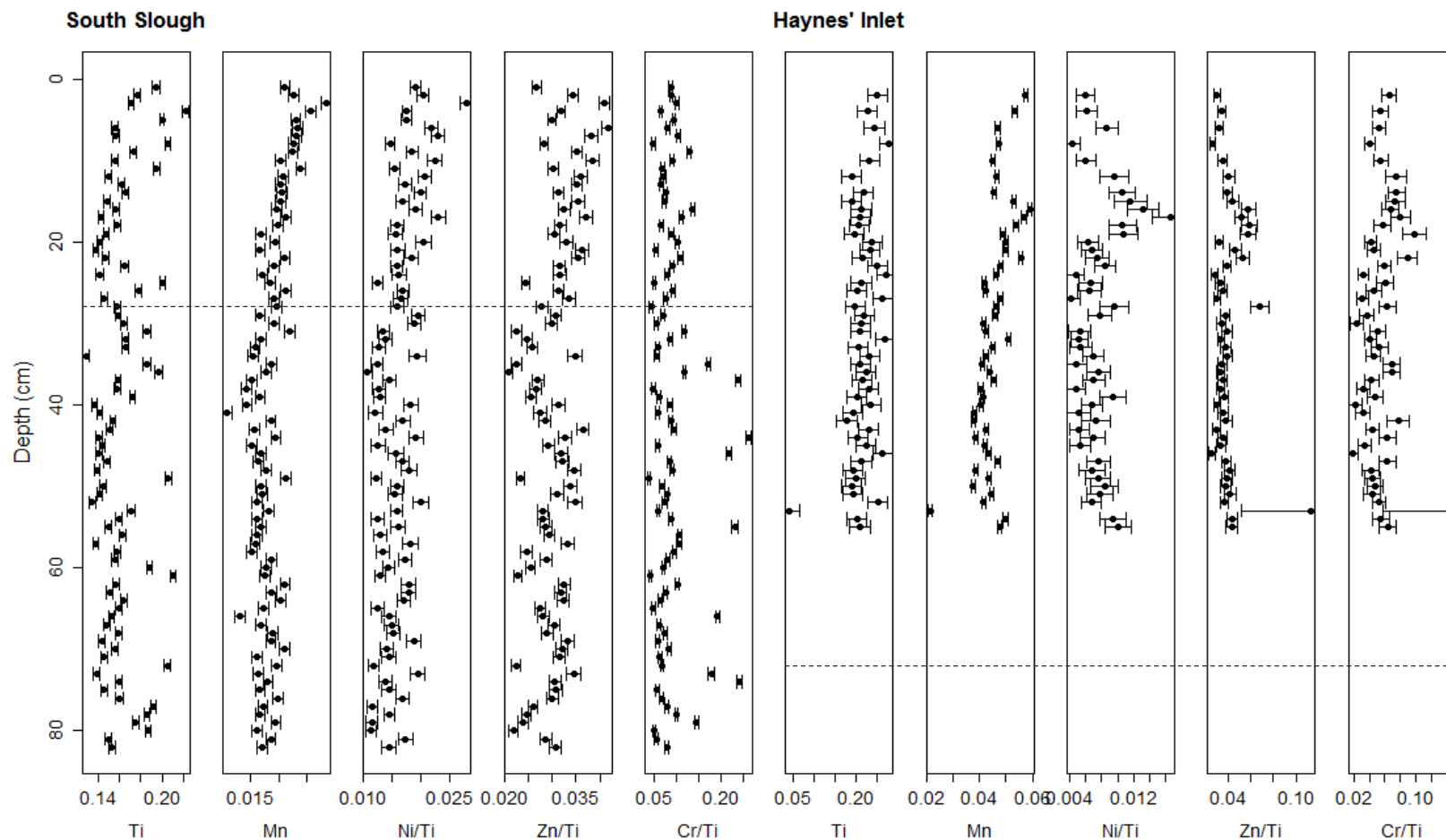


Figure 4. Ti, Mn, Ni, Zn, and Cr in sediment cores from South Slough and Haynes Inlet surface cores. Ti and Mn are pXRF-based estimates of percent mass, whereas of Ni/Ti, Zn/Ti, and Cr/Ti are pXRF-based mass ratios. The horizontal dashed line indicates the depth of ca. 1900 marking the time of increased Euro-American settlement.

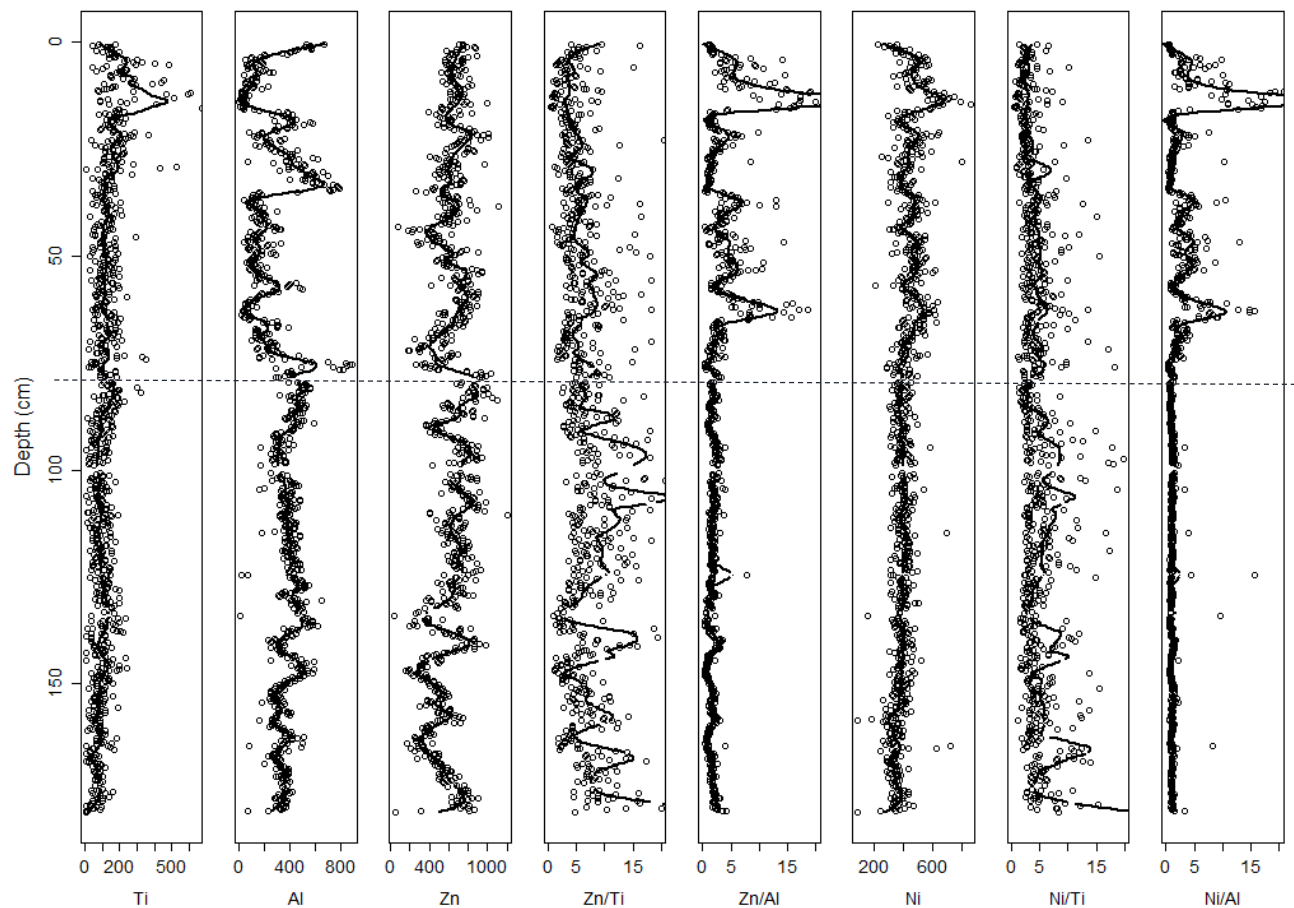


Figure 5 Line-scan XRF: Ti, Al, Ni, and Zn. Elemental proxies of erosion and deposition (Ti, Al), and water quality (Zn, Ni) estimated using 2 mm resolution on split sediment cores from Haynes Inlet. Ni and Zn are expressed as counts per second (cps) and as ratios to Ti and Al. Black lines derived from a loess non-parametric regression. The horizontal dashed line indicates the depth of ca. 1900 marking the time of increased Euro-American development.

### 3.3 Dissolved oxygen observations compared to trace-metal geochemistry

Records from the water quality monitoring station at Valino Island indicate that there has been substantial variation in the prevalence of low DO in the period of record, 1999-2014 (Figure 6). The increase in the duration of low DO during 2004 and 2010 was evident at a low DO threshold of 1 mg/L. At Charleston Bridge, low DO duration peaked in 2006, but was absent otherwise.

There are several notable correlations between elemental fractions of Ti and redox-sensitive metals with observed duration of low DO conditions despite the short monitoring period (Figure 7). First, the variation in redox-sensitive metal concentrations visually matches the DO observations, with similar peaks in anoxia duration and concentration of Ni, Zn, and Cr. Second, temporal and stratigraphic patterns of Ti have a weakly inverse relationship with the duration of anoxia. Normalizing these metals by Ti increases the variability in the trace-metal record and improves its correspondence with the DO record. For example, while bulk Zn lacks a distinct peak near the core top, a peak is observed for Zn/Ti (Figure 7). Similarly, bulk Ni and Zn have smaller peaks in the lower half of this core section, however, they are not perfectly coincident. The effect of normalization creates a single broad peak in both Ni/Ti and Zn/Ti peaks at 2001-2003 and correlate with the observed DO history. Cr/Ti concentrations have no apparent relationship to DO.

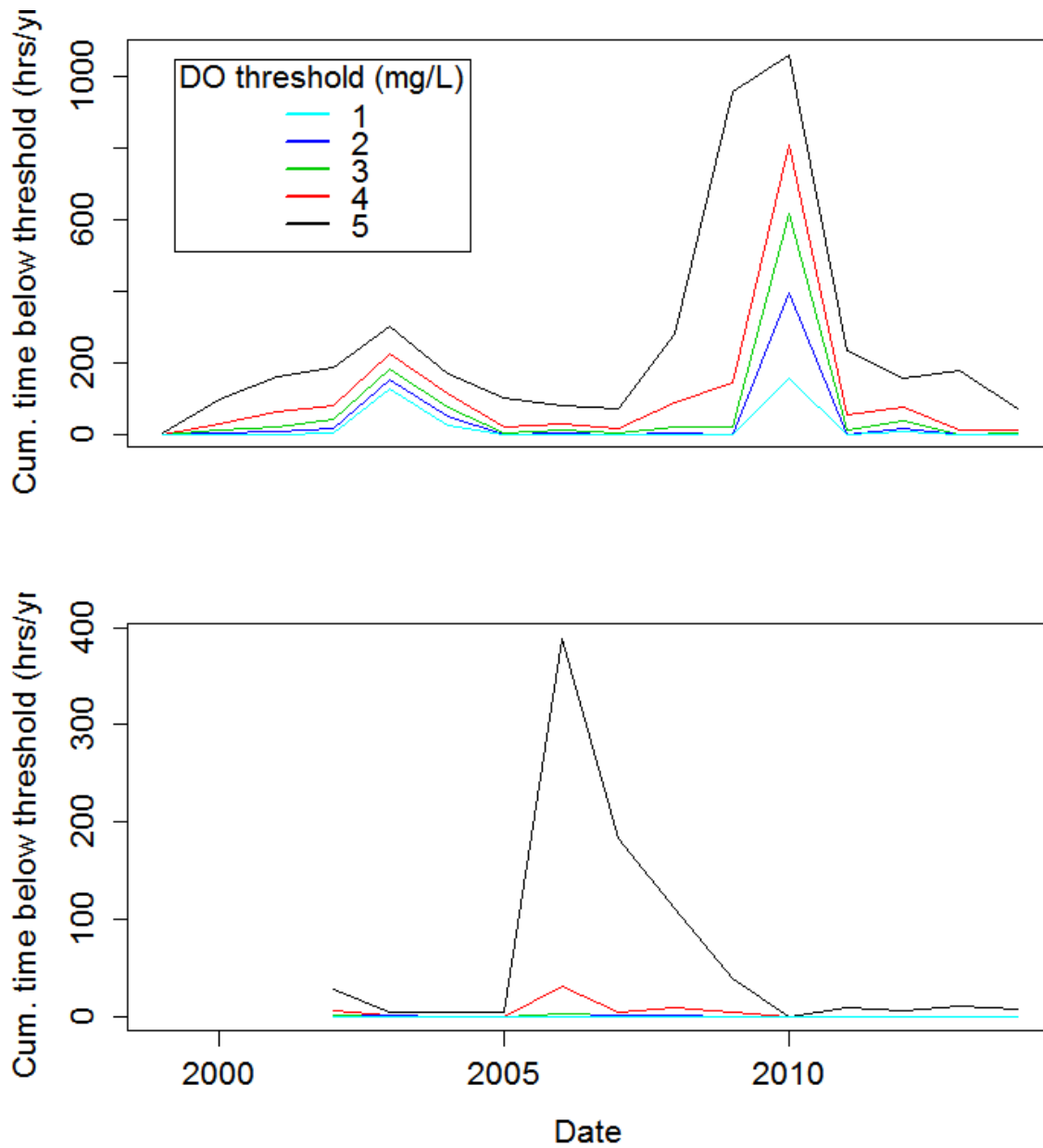


Figure 6. 30-minute water logger data from Valino Island (top) and Charleston Bridge (bottom) summarized as hours per year below DO thresholds of 1-5mg/l. The Valino Island site is closest to SS, and Charleston Bridge is in the dredged channel.

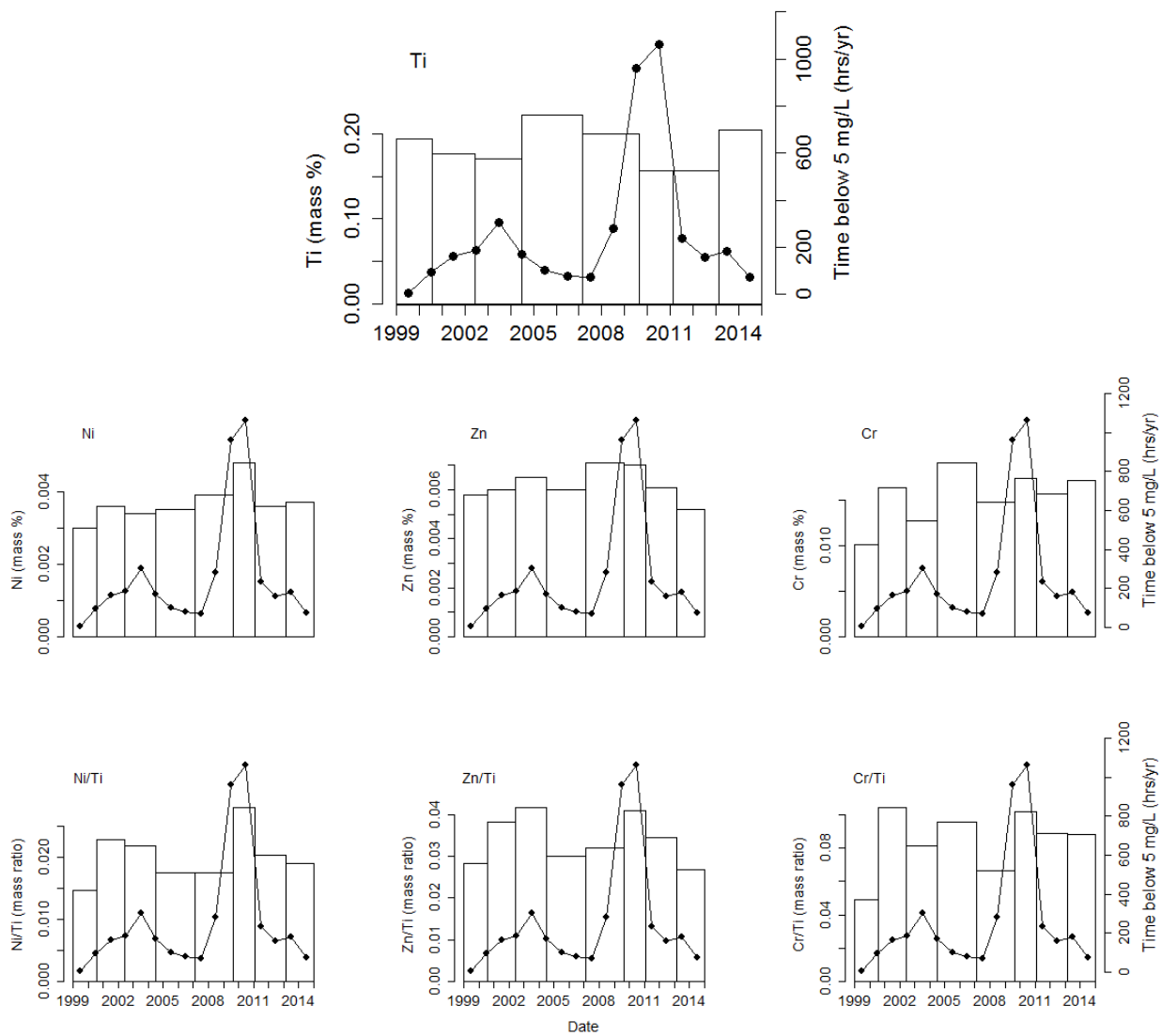


Figure 7. Relationship between Ti erosion proxy with selected trace-metal DO proxies and their relationships to annualized duration of low DO conditions (line) in South Slough at Valino Island.

### **3.4 Pollen proxy of land use and cover change:**

Disturbance-adapted species (Appendix A: Table A1, Figure A1) are the dominant pollen group in the South Slough core, mostly due to high percentages of *Alnus* pollen. The overall trend in the disturbance-adapted pollen group as well as forb-grass pollen and fern spores was a general decrease from 1630 to 1926 ybp. This decrease was followed by an increase in these same pollen and spore categories after 1926. The post-1900 increase is characterized by a more rapid recovery of ferns and grasses, followed by the disturbance-adapted taxa which peaked around 2000 AD. The mid-successional group peaked at 18%, immediately after the decline in disturbance-adapted species. The late-successional taxa group showed little variation over most of the record (39-45%), except for a peak immediately prior to the decline in the disturbance-adapted group (i.e., mid 1800s).

## CHAPTER IV

### DISCUSSION

Strong agreement between geochemical characteristics of sediment cores from South Slough with the measured record of low DO indicate that the redox-sensitive trace metals are sensitive to conditions in the water column over inter-annual and decadal timescales and a detectable record of these metals is preserved in sediment (Figure 7). This finding provides important confirmation that concentrations of redox-sensitive trace metals (especially indicators of eutrophication) indeed reflect the duration of low oxygen conditions in surface waters. This opens the door to reconstructing past variability in DO and thus tracking environmental change in small estuaries, which has never been shown previously. Similar efforts in larger, deeper estuaries have been successful in the Chesapeake Bay (Cronin et al. 2005; Scheiderich et al. 2010) and Hood Canal (Brandenberger et al. 2011).

The pXRF data from South Slough (SS) revealed that the concentration of redox-sensitive metals (Fe, Mn) as well as indicators of eutrophication (Ni, Zn) have been higher in the last 30 years than at any time in the last 335 years. In contrast, at Haynes Inlet (HI), there was little evidence for such an increase in recent decades with the exception of a recent low-DO event that was recorded at both sites. This suggests the importance of a longitudinal gradient within the Coos Bay Estuary (CBE). I propose that the influence of openness to the deeply dredged channel at HI, as opposed to the more isolated SS location, is responsible for this difference between the sites. Sutherland and O'Neill (2016) suggest the deeper, more easily flushed, dredged shipping lane channel has acted as a DO buffer for the main Coos Bay estuary. First I discuss the mechanisms underlying DO variability in the CBE and how they are reflected in the sediment record. Second, I discuss the longer term processes responsible for the increases

in DO proxies in recent decades. Last, I examine the profound increase at both sites in erosion indicators across the settlement horizon (Figure 5).

#### **4.1 Interannual variability in DO and metal concentrations in estuary sediment**

The relatively consistent increase in the concentration of trace metals up to the present at SS is an unusual pattern for estuarine sediment records in developed watersheds, where sediments are often considered contaminant sinks (Ridgway and Shimmiel 2003). More commonly, pollution history studies have found the concentrations of trace metals to peak in the late 1960's and early 1970's prior to environmental regulations (e.g. Valette-Silver 1993, Zwolsmann et al. 1993). The two records analyzed in the CBE, however, appear little affected by industrial pollution (see below). Rather, I found that trace metal concentrations increased throughout the 20<sup>th</sup> century at SS. These increases were paralleled by both bulk organic matter and magnetic susceptibility (Figure 2) suggesting that there has been a recent peak in both supply and preservation of organic matter to this part of South Slough. This increase in organic matter may be the ultimate cause of the increase in the frequency of low DO conditions.

A recent study by Sutherland and O'Neill (2016) found that the dry-season DO status of the CBE is controlled by a combination of stream discharge and tidal forcing. Our results therefore suggest that, on interannual time scales, these short-term processes are mediated by the supply of labile organic matter, likely from phytoplankton production in the water column. Furthermore, in the conceptual model Sutherland and O'Neill propose, biological processes in the water column and an actively respiring upper layer of oxygenated sediment mediate DO status of water supplied predominately from rivers (in winter) or the ocean (in summer). Thus stream and ocean sources provide the supply of oxygenated water and nutrients to the estuarine system but at different seasons.



Little evidence exists of upwelling patterns influencing proxies of DO in the SS or HI cores (Figure 8). While the smaller of the two peaks in the trace metals (Ni/Ti) roughly corresponds to the large upwelling event of 2002, other upwelling events do not match the DO proxy. This is interesting because daily monitoring of nutrient and DO as far as the Sengestacken Arm of the upper South Slough (Figure 1) have been shown to respond to summer-season upwelling as a function of tidal forcing (O'Higgins and Rumrill 2007). Thus our study highlights the differences in the short-term (daily) correlation of individual upwelling events with the DO and nutrient status of bays, estuaries and sloughs versus long-term (aggregated, inter-annual) patterns in prevalence of low-DO inducing conditions.

The other potential control on nutrients and oxygen is the supply of organic matter as controlled by stream processes and land use. However, land use in Coos County as measured by timber harvest is a poor predictor of water quality or sedimentary proxies (Figure 8). A limitation in this comparison is the lack of a spatially precise logging history in the forests proximal to South Slough.

Whether or not land use is responsible for sediment loading, the streams supply organic matter and nutrients to the estuarine system although concentrations may vary seasonally (McConnachie and Petticrew 2006). Stream flow during the entire water year is likely an important control of dry season low-DO potential. In particular, storm events leading to periods of higher than average river discharge during the summer months as in 2010 (Figure 8) might promote low DO conditions in South Slough. Streams provide nutrients for *in situ* autotrophic production and organic matter production. Summer nutrient influxes should most strongly affect estuarine productivity and microbial activity (Canuel and Hardison 2016), while winter storm-

deposited organic matter could have an equally important oxygen demand effect as it decomposes during the following years.

In addition to sediment supply variability, estuarine sedimentation rates are sensitive to changes in mean sea level (MSL) from global climate change (Ruiz-Fernandez et al 2016) and relative sea level (RSL) from coseismic subsidence (e.g. Nelson et al. 1996, Kelsey et al. 1998). Neither of our cores extend to before the 1700 AD subsidence event, but the resulting change in MSL and RSL likely affected sedimentation over the entire length of both cores, which might be a factor causing the high sedimentation rates at both sites.

Decomposition of sediments may release metals back into the water column, therefore affecting the interpretation of DO history. However, if organic matter is buried too quickly to be utilized, metals locked into organic forms and complexes are not released, resulting in an expected correlation of organic matter and elemental proxies (i.e. Ni/Ti and Zn/ Ti). Ni/Ti from SS is only weakly correlated with organic matter estimates from LOI ( $r = 0.39$ ; Figures 2 and 4). At HI, there is no correlation between LOI and Ni/Ti ( $r = -0.17$ ). If preservation of Ni is robust in Coos Bay sediment, then the low correlation between LOI and Ni/Ti indicates Ni preservation on mineral sites post-decomposition. Cored sediment at South Slough and Haynes Inlet had a very shallow oxidized depth; and reducing conditions, seen by ubiquitous sulfate reduction and dark color, predominate below the top 0.5 cm. Both the rapid sedimentation rates and the reducing conditions increase the preservation potential of elemental proxies. Cu, Zn and Ni form sulfides easily (Gooday et al. 2009), which are quite immobile in estuarine sediments (Zwolsman et al. 1993). Organic matter also appears to not limit the concentrations of metals in these sediments despite low (<10%) organic content, thus supporting the conclusion that metal concentrations are correlated with DO conditions in the overlying water.

The general agreement of organic matter and Ni (as opposed to direct correlation) also mitigates concern over the effect of pollution on metal concentrations in the Coos Bay estuary, which can be significant in urbanized estuaries (Zwolzman et al. 1993; Swales et al. 2002; Ridgeway et al. 2003; Morelli et al. 2012). The lack of a substantial increase in metal concentrations at HI (Figure 4), which is much closer to urban centers, also suggests that pollution may not be a significant issue. Furthermore, sediments in the South Slough are generally sourced from its own watershed rather than the main estuary (Wilson et al. 2007). These lines of evidence increase our confidence in the reliability of the sedimentary elemental signature at HI reflecting the greater Coos Bay estuary watershed, while SS better reflects its smaller subwatershed.

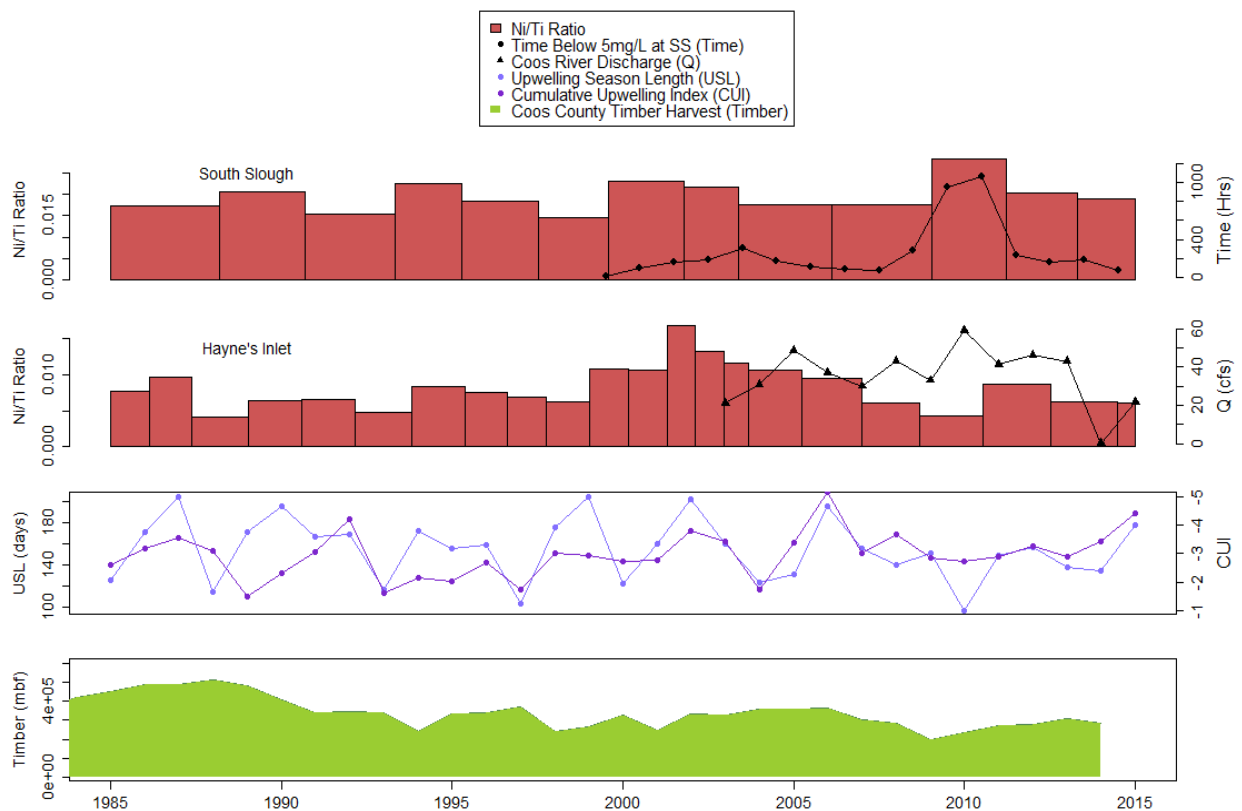


Figure 8. Comparison of the Ni/Ti DO proxy from two core sites and the measured DO at Valino Island with upwelling indices (as a measure of coastal anoxia), median dry season discharge (June – October) of the South Fork Coos River, and timber harvest in the Coos County, OR.

## 4.2 Decoupled processes in the main estuary and the South Slough:

Direct comparison of South Slough and Haynes Inlet is complicated by the substantial difference in temporal resolution between the two cores. Despite this challenge, the HI core shows a similar pattern in elemental composition to the SS core (Figure 8). Interestingly, the variability in Ni/Ti is substantially lower in the HI than SS, which suggests that the distribution of conditions that promote low DO in the estuary vary by location in the estuary. DO near the ocean is highest when river discharge is low during the summer dry season (Sutherland and O'Neill 2016). At interannual to decadal time scales, summer discharge of the Coos River (which feeds the main estuary) does not seem to play an important a role in creating low DO conditions in the South Slough (Figure 8). This lack of correspondence may be due to the smaller watershed of the South Slough compared to the entire CBE. However, the highest South Fork Coos River discharge during the summer of 2010 (Figure 8) corresponds to the highest peak in Ni/Ti and a minimum in DO at SS. This correspondence could be related to summer organic matter delivery (McConnachie and Petticrew 2006), which would be particularly available to aerobic pathways during warm summer months. In the main estuary summer discharge of the Coos and Millicoma rivers, even during drier than average summers, is sufficient to replenish the relatively deep, high-volume DO reservoir in the dredged main channel (Sutherland and O'Neill 2016). South Slough, however, joins the CBE close to the coast and is not greatly affected by main-channel waters (Rumrill 2006; Sutherland and O'Neill 2016). Rather, the South Slough's shallower channel and small watershed lead to highly seasonal hydrographic dynamics. Generally, there is a well-mixed water column during the low river discharge in summer when DO is higher near the ocean, and a more thoroughly stratified salt-wedge in the winter with cold, high DO, low salinity water up-estuary (Sutherland and O'Neill 2016). This is more similar than

the HI site to other small estuaries in Oregon, Washington, and California without dredged channels (e.g. Brown and Power 2011).

In contrast to South Slough, the Haynes Inlet site is more open to the main estuary (Figure 1). Much higher average sediment accumulation rates at this mid-estuary position are likely due to storm-deposited sediment falling out of suspension in the deeper, calmer water of the main estuary, a pattern also observed by Swales et al. (2002) in Pakuranga estuary, New Zealand and Ralston and Geyer (2009) in the Hudson River estuary. At HI, the high-resolution (2mm) core-scanning data and higher sedimentation rate also shed light on the frequency and composition of high discharge, storm-driven, deposition. Our results add a decadal to centennial perspective to storm-driven depositional events. In particular, large storm events in 2005, 1996, 1964 and 1861 (Wallick et al. 2011) are apparent in the HI core. The sand layer of the 1964 storm (starting at 40 cm) is over 5 cm thick in contrast to most other sand layers in the core (Figure 2), while the only other sand layer of similar thickness correlates with the storm of 1868 (90cm). Below the 1964 storm strata, there are numerous sandy lenses, though none is as large as 1964 and 1868. The last visible sand layer occurred at ca. 1964 (Figure 2), although sedimentation rate continued to increase to the present (Figure 3). A similar trend is evident from the SS core as well. The increase in sedimentation may be due to fine sediment loading from forest harvest that peaked in the 1960's (Ringler and Hall 1975; Sedell et al. 1991). The absence of a sandy lens at the time of the 2005 and 1996 storms is not explained.

Our qualitative grain-size evidence (Figure 2) of an effect from the post-settlement disturbances is corroborated by estimates of organic matter from LOI (Figure 3) and the core-scanning XRF (Figure 5). In the upper half of the HI core, these measures reveal instantaneously deposited sand layers alternating with the more slowly accumulated material. In the lower half of

the core, roughly corresponding to the pre-settlement era, there is a signature in erosion indicators (Al and Ti) of higher background disturbance rate (higher frequency, lower magnitude), punctuated by narrower, less intense peaks than in the post-settlement era (Figure 5). In addition, sedimentation rates have increased over the past 100 years. Al (and K, which was highly correlated with Al in the HI core) – proxies of chemical weathering and fine sediment deposition in the form of alumino-silicates and feldspar respectively – exhibit this changing depositional pattern well. Both Al and K were relatively less variable pre-settlement, indicating less variable sedimentation rates (Figure 5). Post-settlement, much lower baseline counts for these elements are punctuated by high-magnitude peaks in the post-storm-flow sedimentation events after 1964, 1978, and 1996. This suggests an increase in storm deposition accompanied by a reduction in sorting of fine and coarse fractions. This agrees with Miller's (2010) assessment of the splash dam-induced stream simplification legacies leading to reduced sediment storage in the stream system, combined with the increased availability of fine sediment from upland logging-induced erosion (Brown and Krygier 1971). Stream simplification allows rapid transport of storm-eroded material thus potentially flushing erodible material and leaving the stream system with reduced sediment storage. Thus a more stochastic sedimentation regime could be responsible for the low Al baseline in the post-settlement era.

In comparison to Al and K, Ti variability shows a large range in only the top 30cm, yet similarities with Al and K do exist. Many previous studies interpret Ti as a proxy of upland erosion from physical weathering processes in comparison to the Al-K proxies (e.g. Brown 2011; Arnaud et al. 2015). In the Oregon Coast Range, uplift is roughly balanced by erosion (Reneau and Dietrich 1991, Roering et al. 2001), which is primarily in the form of debris flows triggered almost exclusively by unusually high precipitation events (Benda and Cundy 1990). Typically,

the highly heterogeneous upland sediment (organic and mineral) supplied to stream channels by this process persists for 10-20 years before diffusion downstream (Miller 2010). While the Ti record at both sites show discrete peaks related to such events, the most notable occurs at the core top at HI, suggesting the possibility of a uniquely severe, stochastic upland erosion pattern within the last 50-60 years.

#### 4.3 Long-term proxies of water quality and human landscape effects in PNW estuaries:

Long-term Ni/Ti reconstruction (Figure 9) from the SS core shows a substantial increase after 1900 relative to pre-settlement, indicating that the environmental conditions shown to promote low-DO in the South Slough may have been less prevalent pre-Euro-American settlement.

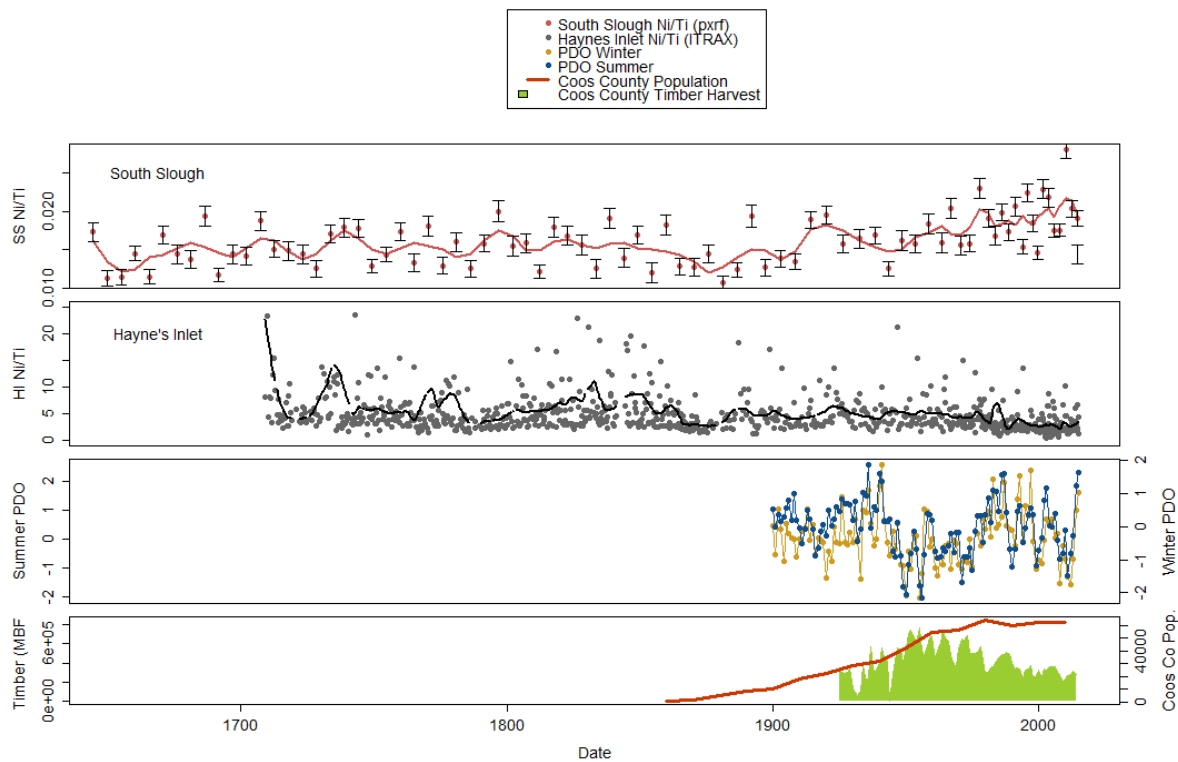


Figure 9. Long-term synthesis of anthropogenic and climatic forcings alongside Ni/Ti from pXRF (SS) and core-scanning XRF-measured Ni/Ti (HI). PDO indices from Mantua (2016). Coos County logging records extend back only to 1930 (Andrews and Kutara 2005).

This increase coincides well with the onset of the extensive forest clearance of the first half of the 20<sup>th</sup> century (Lansing 2005, 2007) as well as the draining and diking of salt marsh and mudflats for agricultural purposes (Cornu 2005). The reduction of timber harvest after 1970 (Andrews and Kutara 2005; Figure 9), however, is not represented by a reduction in Ni/Ti, thus the magnitude of harvest does not appear to provide satisfactory explanation for the continued increase of these proxies. It is possible that the organic loading effect of upland erosion may have been compounded by increasing wastewater pollution as the local population grew. However, the installation of water treatment facilities beginning as early as 1954 along the CBE (Brown and Power 2011) is also not reflected in rising Ni/Ti at SS but is consistent with declining Ni/Ti at HI. At HI, Ni from core-scanning (ITRAX) XRF does register an increase in the magnitude of periodic peaks after 1900 AD (Figure 5), however, Ni/Ti indicates an overall reduction in the relative amount of allochthonous Ni in sediment over the last 270 years, and especially in the last 100 years (Figure 9). Increasing Ni and Ti suggests that Ni has an upland source or its preservation is enhanced by the addition of upland components due to coincidence of bulk Ni increase with Ti and Euro-American landscape modification. Zn variability, however, does not change from pre-to-post-settlement suggesting different Zn and Ni sources.

#### **4.4 Geochemical proxies from pre- to post-settlement.**

Prior to Euro-settlement a parallel trend in geochemical proxies from SS and HI cores may yield some insight into the landscape effects of the transition from Native American to Euro-American land use regimes. From the 1730s until after 1800 AD (120cm), Ni increases steadily with low variability while Zn shows an overall increase with greater variability (Figure 5), indicating a slow increase in potential water column oxygen stress from nutrient and organic matter loading. Ti and Al both increase over the same time period, then decrease until ca. 1900



AD (80cm). These erosion indicators further suggest enhanced upland disturbance and sediment delivery.

The SS core follows a similar pattern despite differences in the age-depth relationship at this site. Higher concentrations of Ni and other metal indicators prior to 1800 AD (55cm) were followed by a reduction of sedimentation rates and low-DO proxies (Figures 2 and 4). This relaxation was followed by the onset of the dramatic post-settlement increases in erosion starting in ca. 1900 (28cm), and the resulting potential for water column DO stresses (Figures 5 and 9).

Although other explanations may be invoked (e.g. climate variability or variability in shallow land sliding), the timing of these changes are consistent with changing land use through the settlement period. In particular, the decreases in geochemical proxies of erosion 50-60 years prior to extensive Euro-American settlement beginning about 1800 AD in both SS and HI cores agrees with the documented decline of Coos peoples living along the shores of the CBE. First peoples in the Coos region experienced catastrophic population losses from repeated measles and small-pox epidemics following the earliest contact with French and Dutch trappers in the 1820s and 30s (Douthit 1999). Rough estimates from anecdotal evidence suggest a Coos population of 2000-3000 people, steadily increasing, existed prior to the epidemics (Erlandson et al. 2008). The pervasive use of fire as a game management strategy in the watershed (Lansing 2005, Youst 1997), was likely a long-term cultural norm, and the high-frequency low intensity disturbance regime inferred at SS and HI sites is consistent with this hypothesis. Larger wildfires can also effect watershed processes dramatically, and a large fire burned more than 90,000 ha in the 1850s at what is now the Elliot State Forest (Leiburg 1900). Little evidence of substantial effects from this event could be attributed to the higher overall fire activity at that time.

#### **4.5 Climate, pollen and land use and cover change 1630-present.**

At the edge of the mudflat below water, tidal energy and sorting processes resulted in very low pollen concentration in the SS core, similar to other active estuarine sediments (Gastaldo et al. 2012; Chmura and Eisma 1995). However, pollen spectra represent a unique tool to understand the pre-settlement environment and disturbance regime (Swales et al. 2002; Yang et al. 2014). Pollen evidence of landscape modification from South Slough also corroborates the concept of Coos land management ecological impacts and the post-settlement regime developed above with geochemical evidence. High counts of disturbance-adapted pollen in the lower portion of the SS core – late-1600s to early 1800s – are followed by a steady reduction until the early 1900s. Extensive logging did not begin until the 20<sup>th</sup> century and is associated with increases in representation of disturbance-adapted taxa. Mid-successional species reached their peak during the lowest period of disturbance, which would be expected as populations of fire-sensitive *Picea* and *Pinus* were able to increase in abundance. The late successional group did not change greatly, although an increase in pollen representation coincident with the decline of disturbance-adapted species after 1800 agrees with geochemical evidence (above) of a lag between the relaxation of Native American disturbance regime and regrowth of the forest margin.

On centennial time-scales (Figure 9), I contrasted anthropogenic effects (pre- and post-settlement) with climatic forcing mechanisms represented here as the Pacific Decadal Oscillation (PDO), an index of sea-surface temperature with long-term reconstruction from regional meteorological measurements (Zhang et al. 1997, Mantua 2016). PDO reflects patterns in precipitation (and thus river discharge) as well as the prevalence of coastal fog and potential evapotranspiration which also affect ecohydrological patterns over multiple timescales. On the

Oregon Coast, cool PDO corresponds to increased winter precipitation and increased drought, whereas warm PDO decreased winter precipitation and drought (Goodrich 2007). A strong cool phase of the PDO occurred from 1947 to 1954 and corresponds with lower Ni/Ti values at SS, which is a notable departure from the long-term increase in Ni/Ti from 1900 AD onward. The subsequent return to a PDO warm phase by 1976 also tracks the Ni/Ti at SS, and higher PDO since then agrees with higher Ni/Ti. To a lesser extent, the HI surface core data demonstrate this pattern as well, the lowest sustained Ni/Ti at 30-45 cm (1945-1975). In general, this agrees with my assessment of modern hydrological influence which suggests that summers with higher river discharge (low drought, warm PDO) are more likely to experience low DO conditions. From these observations I suggest a regional climatic influence (e.g. PDO) on hydrological patterns is also reflected in the sedimentary record of low DO conditions.

Interestingly, the other common inference of modern California Current System upwelling and sea-surface temperature patterns is directly related to the establishment of terrestrial ecological patterns in the Oregon Coast Range. Millennial reconstructions indicate that long-term upwelling patterns are also related to coastal fog and the prevalence of fire and establishment of *Picea* forests (Long and Whitlock 2002) as well as the California Current System dynamics (Pisias et al. 2001). Thus a climate history of upwelling is also potentially a record of estuarine water quality especially in the near-ocean part of the estuary. On these millennial time scales, river discharge, upwelling, precipitation, and sea surface temperatures are likely to be additional important factors driving DO conditions.

## **CHAPTER V**

### **CONCLUSIONS**

The relatively recent installation of water monitoring equipment in Coos Bay limits our understanding of trends in environmental conditions to only the recent past. Analysis of sedimentary proxies offers a long-term perspective on current concerns about estuarine water quality. Our analysis of geochemical proxies for organic matter loading, erosion, and redox-sensitive metals from the Coos Bay Estuary complex indicates that estuary sediments preserve a record of interannual-to-decadal variability in water quality. Furthermore, centennial scale variations in these proxies reflect land use and cover change through the history of Native American land stewardship practices and Euro-American settlement and development. Additionally, trends in Pacific climate indices (e.g. PDO) may play an important role in establishing decadal DO trends.

Our geochemical proxies suggest that periods of low DO are greater in the more isolated South Slough over the past several decades compared to any time of the past 335 years. The most likely explanation for the increased oxygen stress is increased organic matter loading. Conversely, the mid-estuary (Haynes Inlet) site's openness to the main estuary may buffer watershed impacts on DO status. At this site, organic matter and geochemical proxies have stayed relatively stable or decreased. Erosion indicators show a distinct signal of greater magnitude erosion events, but decreased frequency, following Euro-American settlement.

These results add a decadal to centennial perspective to the conceptual model of Sutherland and O'Neill (2016) which highlights the importance of the CBE's dredged channel to maintaining relatively stable DO conditions in the main estuary even during summer months due to openness to the oceanic DO pool. The differences between the two core sites are consistent

with the role of the connection to the main channel: The South Slough site was affected to a greater extent by local watershed disturbances likely in part due to the lack of a deeply dredged channel, while the mid-estuary site is more open to the dredged channel and buffering effects of ocean-driven tides. In addition, there was similarity between the sites on annual scales as a recent period of extended low DO conditions appears to have occurred at both sites.

Our results strengthen the case for reinforcing water quality monitoring programs in estuarine and coastal environments to maintain the temporal density of environmental knowledge. In particular, long, continuous records are critical to making sense of paleoenvironmental proxies for water quality. Fortunately, geochemical proxies of past environments and processes offer the prospect of extending our knowledge well beyond the measurement record. Unfortunately, widespread use of these techniques to map the spatial and temporal characteristics of water quality, not to mention myriad other environmental phenomena, has been hampered by time and expensive analytical techniques (e.g. mass spectrometry). PXRF (as well as modern benchtop XRF) and core-scanning XRF now potentially offer long-term perspectives on estuarine processes to watershed groups or local communities seeking sustainable solutions to conflicts between land-use interests and natural resource longevity and reliability.

## APPENDICES

### APPENDIX A. POLLEN FIGURES AND TABLES

Table A1. Pollen Functional Groups

Disturbance adapted	Mid-successional	Late successional	Forb/Grass
<i>Alnus</i>	<i>Pinus</i>	<i>Tsuga</i>	<i>Ericaceae</i>
<i>Corylus</i>	<i>Picea</i>	<i>Cupressaceae</i>	<i>Myrica</i>
<i>Salix</i>		<i>Abies</i>	<i>Chenopodiaceae</i>
<i>Pseudotsuga</i>		<i>Taxus</i>	<i>Oxalis</i>
<i>Populus</i>		<i>Sapindaceae</i>	<i>Rosacea</i>
<i>Fraxinus</i>		<i>Betula</i>	<i>Brassicaceae</i>
			<i>Asteraceae</i>
			<i>Ranunculus</i>
			<i>Penstemon</i>
			<i>Typhaceae</i>
			<i>Poaceae</i>
			<i>Cyperaceae</i>

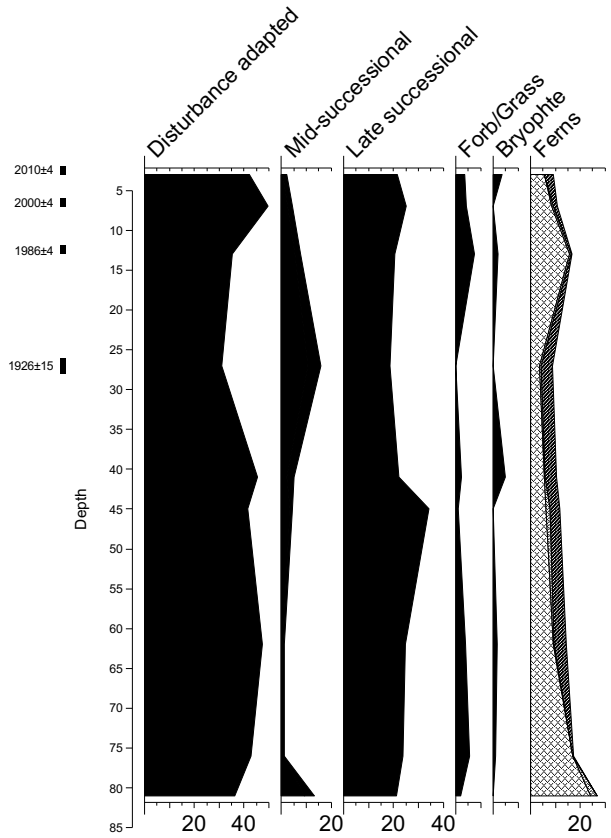


Figure A1. Pollen percentages by disturbance adaptation groups.

## APPENDIX B. USACE DREDGING RECORDS: 1855-2015 CE

The following is obtained from a Freedom of Information Act request for Coos Bay dredging spoils areas and volumes from 1950- 2015, which returned a record from 1976-2015.

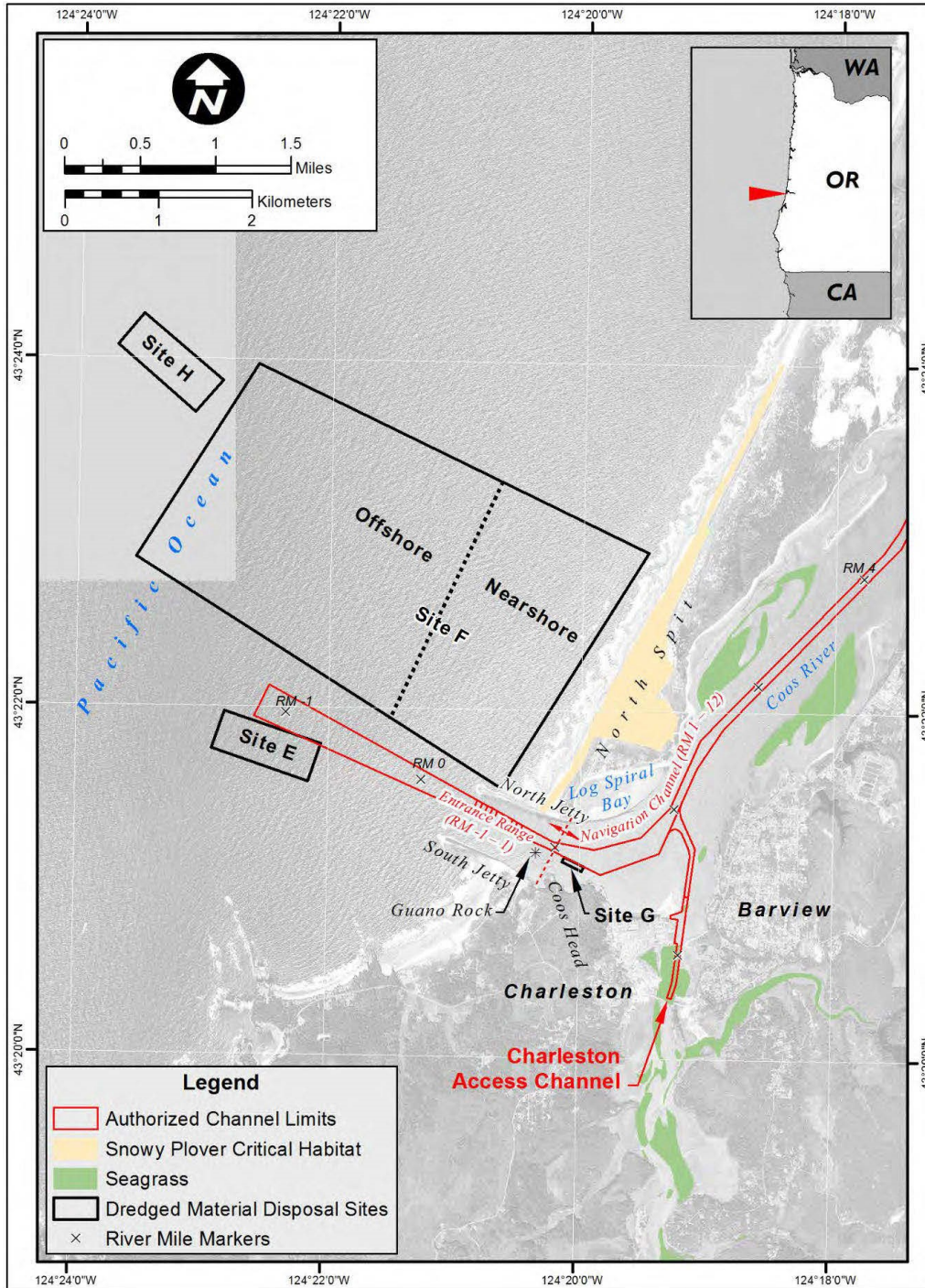


Figure B1. Vicinity Map – Lower Coos Bay and Coastal Offshore Project Area (USACE 2015).

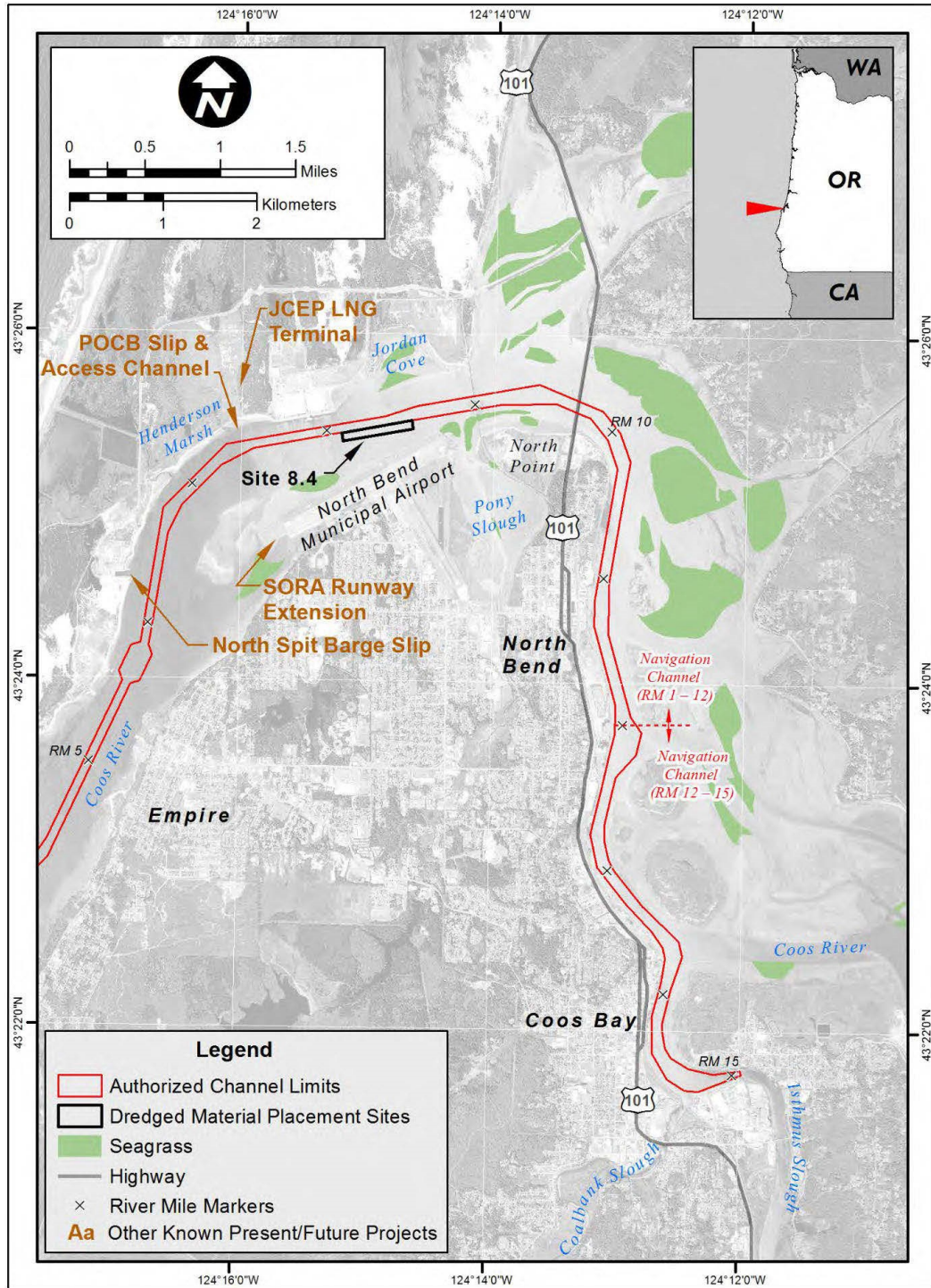


Figure B2. Vicinity Map – Upper Coos Bay Project Area (USACE 2015).



## REFERENCES CITED

- Adelson, J. M., Helz, G. R., & Miller, C. V. (2001). Reconstructing the rise of recent coastal anoxia; molybdenum in Chesapeake Bay sediments. *Geochimica et Cosmochimica Acta*, 65(2), 237–252. [http://doi.org/10.1016/S0016-7037\(00\)00539-1](http://doi.org/10.1016/S0016-7037(00)00539-1)
- Andrews, Alicia, and Kristin Kutara. 2005. “Oregon’s Timber Harvests: 1849-2004.” Salem, Or. [http://www.oregon.gov/odf/state\\_forests/frp/docs/oregonstimmerharvests.pdf](http://www.oregon.gov/odf/state_forests/frp/docs/oregonstimmerharvests.pdf).
- Appleby, P.G., and F. Oldfield. 1978. “The Calculation of Lead-210 Dates Assuming a Constant Rate of Supply of Unsupported  $^{210}\text{Pb}$  to the Sediment.” *Catena* 5 (1): 1–8. doi:10.1016/S0341-8162(78)80002-2.
- Arnaud, F., Révillon, S., Debret, M., Revel, M., Chapron, E., Jacob, J., Magny, M. (2012). Lake Bourget regional erosion patterns reconstruction reveals Holocene NW European Alps soil evolution and paleohydrology. *Quaternary Science Reviews*, 51, 81–92. <http://doi.org/10.1016/j.quascirev.2012.07.025>
- Barbier, E. B., Hacker, S. D., Kennedy, C., Koch, E. W., Stier, A. C., & Silliman, B. R. (2011). The value of estuarine and coastal ecosystem services. *Ecological Monographs*, 81(2), 169–193. doi:10.1890/10-1510.1
- Barron, John A., and David Bukry. 2007. “Development of the California Current during the Past 12,000 yr Based on Diatoms and Silicoflagellates.” *Palaeogeography, Palaeoclimatology, Palaeoecology* 248 (3-4): 313–338. doi:10.1016/j.palaeo.2006.12.009.
- Binford, M. W. (1990). Calculation and uncertainty analysis of  $^{210}\text{Pb}$  dates for PIRLA project lake sediment cores. *Journal of Paleolimnology*, 3, 253–267.
- Blaauw, M., Christen, J.A., 2011. Flexible paleoclimate age-depth models using an autoregressive gamma process. *Bayesian Analysis* 6, 457-474
- Brandenberger, J. M., Louchouart, P., & Crecelius, E. A. (2011). Natural and Post-Urbanization Signatures of Hypoxia in Two Basins of Puget Sound: Historical Reconstruction of Redox Sensitive Metals and Organic Matter Inputs. *Aquatic Geochemistry*, 17, 645–670.
- Brown, G. W., & Krygier, J. T. (1971). Clear-Cut Logging and Sediment Production in the Oregon Coast Range. *Water Resources Research*, 7(5), 1189–1198. <http://doi.org/10.1029/WR007i005p01189>

- Brown, Cheryl a., and James H. Power. 2011. "Historic and Recent Patterns of Dissolved Oxygen in the Yaquina Estuary (Oregon, USA): Importance of Anthropogenic Activities and Oceanic Conditions." *Estuarine, Coastal and Shelf Science* 92 (3): 446–455. doi:10.1016/j.ecss.2011.01.018.  
<http://dx.doi.org/10.1016/j.ecss.2011.01.018>.
- Brown, E. T. (2011). Lake Malawi's response to "megadrought" terminations: Sedimentary records of flooding, weathering and erosion. *Palaeogeography, Palaeoclimatology, Palaeoecology*, 303(1-4), 120–125.  
<http://doi.org/10.1016/j.palaeo.2010.01.038>
- Brush, G. S. (2009). Historical land use, nitrogen, and coastal eutrophication: A paleoecological perspective. *Estuaries and Coasts*, 32(1), 18–28.  
<http://doi.org/10.1007/s12237-008-9106-z>
- Canuel, E. A., & Hardison, A. K. (2016). Sources, Ages, and Alteration of Organic Matter in Estuaries. *Annual Review of Marine Science*, 8(1), annurev-marine-122414-034058. <https://doi.org/10.1146/annurev-marine-122414-034058>
- Chan, F, J Barth, J Lubchenco, A Kirincich, H Weeks, W T Peterson, and B Menge. 2008. "Emergence of Anoxia in the California Current Large Marine Ecosystem." *Science* 319 (February): 920. doi:10.1126/science.1149016.
- Chmura, G. L., and D. Eisma. 1995. "A Palynological Study of Surface and Suspended Sediments on a Tidal Flat: Implications for Pollen Transport and Deposition in Coastal Waters." *Marine Geology* 128: 183–200. doi:10.1016/0025-3227(95)00096-H.
- Colman, Steven M., Pattie C. Baucom, John F. Bratton, Thomas M. Cronin, John P. McGeehin, Debra Willard, Andrew R. Zimmerman, and Peter R. Vogt. 2004. "Radiocarbon Dating, Chronologic Framework, and Changes in Accumulation Rates of Holocene Estuarine Sediments from Chesapeake Bay." *Quaternary Research* 61 (2): 241. doi:10.1016/j.yqres.2003.11.004.
- Cornu, C.E. 2005. Restoring Anderson Creek Marsh. South Slough NERR Coastal Resource Management Series. CRMS-200-3. Coos Bay, Oregon.
- Cronin, T. M., Thunell, R., Dwyer, G. S., Saenger, C., Mann, M. E., Vann, C., & Seal, I. R. (2005). Multiproxy evidence of Holocene climate variability from estuarine sediments, eastern North America. *Paleoceanography*, 20(4).  
<http://doi.org/10.1029/2005PA001145>
- Dean, W. E., Zheng, Y., Ortiz, J. D., & van Geen, A. (2006). Sediment Cd and Mo accumulation in the oxygen-minimum zone off western Baja California linked to global climate over the past 52 kyr. *Paleoceanography*, 21(4), 1–13.  
<http://doi.org/10.1029/2005PA001239>

- Dicken, S. N., & Dicken, E. F. (1979). *The making of Oregon: a study in historical geography*. BOOK, Portland, Or.: Oregon Historical Society.
- Douthit, N. (1999). *A Guide to Oregon South Coast History*. Corvallis, OR: Oregon State University Press.
- Eakins, J. D. & Morrison R. T. (1978). A new procedure for the determination of lead-210 in lake and marine sediments. *International Journal of Applied Radiation and Isotopes*, 29, 531-536.
- Erlandson, J. M., Moss, M. L., & Des Lauriers, M. (2008). Life on the edge: early maritime cultures of the Pacific Coast of North America. *Quaternary Science Reviews*, 27(23–24), 2232–2245. <https://doi.org/10.1016/j.quascirev.2008.08.014>
- Faegri, K., Kaland, P. E., & Krzywinski, K. (1989). *Textbook of pollen analysis* (4th ed.). BOOK, Chichester [England]: Chichester England.
- Gooday, A. J., Jorissen, F., Levin, L. a., Middelburg, J. J., Naqvi, S. W. a., Rabalais, N. N., ... Zhang, J. (2009). Historical records of coastal eutrophication-induced hypoxia. *Biogeosciences*, 6(8), 1707–1745. <https://doi.org/10.5194/bg-6-1707-2009>
- Gastaldo, R. A. (2012). Taphonomic controls on the distribution of palynomorphs in tidally influenced coastal deltaic settings. *Palaios*, 27(11), 798–810. <https://doi.org/10.2110/palo.2012.p12-030r>
- Goodrich, G. B. (2007). Influence of the Pacific Decadal Oscillation on Winter Precipitation and Drought during Years of Neutral ENSO in the Western United States. *Weather and Forecasting*, 22(1), 116–124. <http://doi.org/10.1175/WAF983.1>
- Heiri, Oliver, André F. Lotter, and Gerry Lemcke. 2001. “Loss on Ignition as a Method for Estimating Organic and Carbonate Content in Sediments: Reproducibility and Comparability of Results.” *Journal of Paleolimnology* 25 (1): 101–110. doi:10.1023/A:1008119611481.
- Huppert, D. D., Johnson, R. L., Leahy, J., & Bell, K. (2003). Interactions between human communities and estuaries in the Pacific Northwest: Trends and implications for management. *Estuaries*, 26(4), 994–1009. <http://doi.org/10.1007/BF02803359>
- Kelsey, H. M., Witter, R. C., & Hemphill-Haley, E. (1998). Response of a small Oregon estuary to coseismic subsidence and postseismic uplift in the past 300 years. *Geology*, 26(3), 231–234.

- Kenna, T. C., Nitsche, F. O., Herron, M. M., Mailloux, B. J., Peteet, D., Sritairat, S., ... Baumgarten, J. (2011). Evaluation and calibration of a Field Portable X-Ray Fluorescence spectrometer for quantitative analysis of siliciclastic soils and sediments. *Journal of Analytical Atomic Spectrometry*, 26(2), 395. <https://doi.org/10.1039/c0ja00133c>
- Lansing, W. A. (2005). *Seeing the forest for the trees*. Eugene, OR: The Monroe Press.
- Lansing, William A. (2007). *Can't you hear the whistle blowing: Logs, lignite and locomotives of Coos County, Oregon*. Eugene, OR: The Monroe Press.
- Leiberg John B. (1900). *The Cascade Range and Ashland forest reserves and adjacent regions*. Washington: Gov't Print Off. Retrieved from <http://www.biodiversitylibrary.org/item/92325>
- Mathabane, N. (2015). *Potential impacts of timber harvesting, climate and conservation on sediment accumulation and dispersal in the South Slough National Estuarine Research Reserve, Oregon*. University of Oregon. <https://doi.org/10.1017/CBO9781107415324.004>
- Mathieu, G.G., Biscaye P.E., Lupton R.A. and Hammond D.E. (1988). System for measurement of  $^{222}\text{Rn}$  at low levels in natural waters. *Health Physics* 55, 989 – 992.
- Mantua, N. (2016). The Pacific Decadal Occillation (PDO). Retrieved September 9, 2016, from <http://research.jisao.washington.edu/pdo/>.
- McConnachie, J. L., & Petticrew, E. L. (2006). Tracing organic matter sources in riverine suspended sediment: Implications for fine sediment transfers. *Geomorphology*, 79(1-2), 13–26. <http://doi.org/10.1016/j.geomorph.2005.09.011>
- Moore, D. M., & Reynolds, R. C. (1997). *X-ray diffraction and the identification and analysis of clay minerals* (2nd ed.). Oxford: Oxford University Press.
- Miller, R. R. (2010). Is the Past Present? Historical Splash-dam Mapping and Stream Disturbance Detection in the Oregon Coastal Province. Master's Thesis. Oregon State University. <http://doi.org/10.1017/CBO9781107415324.004>
- O'Higgins, T., & Rumrill, S. S. (2007). *Tidal and Watershed Forcing of Nutrients and Dissolved Oxygen Stress within Four Pacific Coast Estuaries: Analysis of Time-Series Data collected by the National Estuarine Research Reserve System-Wide Monitoring Program (2000-2006) within Padilla Bay (WA)*. The NOAA/UNH Cooperative Institute for Coastal and Estuarine Environmental Technology (CICEET). <https://doi.org/10.1017/CBO9781107415324.004>

- Nelson, A. R., Jennings, A. E., & Kashima, K. (1996). An earthquake history derived from stratigraphic and microfossil evidence of relative sea-level change at Coos Bay, southern coastal Oregon. *Bulletin of the Geological Society of America*, 108, 141–154. [https://doi.org/10.1130/0016-7606\(1996\)108<0141:AEHDFS>2.3.CO;2](https://doi.org/10.1130/0016-7606(1996)108<0141:AEHDFS>2.3.CO;2)
- O'Neill, M. A. (2014). *Seasonal hydrography and hypoxia of Coos Bay, Oregon*. University of Oregon.
- Peterson, Emil R. (1952). *A Century of Coos and Curry: History of Southwest Oregon*. Portland, Or.: Portland, OR.: Binfords & Mort for Coos-Curry Pioneer and Historical Association, Coquille.
- R Core Team. (2015). R: A language and environment for statistical computing. R Foundation for Statistical Computing, Vienna, Austria. Available at <https://www.R-project.org/>.
- Ralston, D. K., & Geyer, W. R. (2009). Episodic and long-term sediment transport capacity in The Hudson River estuary. *Estuaries and Coasts*, 32(6), 1130–1151. <http://doi.org/10.1007/s12237-009-9206-4>
- Reneau, S. L., & Dietrich, W. E. (1991). Erosion rates in the southern oregon coast range: Evidence for an equilibrium between hillslope erosion and sediment yield. *Earth Surface Processes and Landforms*, 16, 307–322. <http://doi.org/10.1002/esp.3290160405>
- Ridgway, J., & Shimmield, G. (2002). Estuaries as Repositories of Historical Contamination and their Impact on Shelf Seas. *Estuarine, Coastal and Shelf Science*, 55(6), 903–928. <https://doi.org/10.1006/ecss.2002.1035>
- Ruiz-Fernandez, A. C., Sanchez-Cabeza, J.-A., Serrato de la Pena, J. L., Perez-Bernal, L. H., Cearreta, A., Flores-Verdugo, F., Diaz-Asencio, M. (2016). Accretion rates in coastal wetlands of the southeastern Gulf of California and their relationship with sea-level rise. *The Holocene*. <http://doi.org/10.1177/09596836166632882>
- Rumrill, S. S. (2007). *The Ecology of the South Slough Estuary: Site Profile of the South Slough National Estuarine Research Reserve*. Charleston, OR.
- Scheiderich, K., Helz, G. R., & Walker, R. J. (2010). Century-long record of Mo isotopic composition in sediments of a seasonally anoxic estuary (Chesapeake Bay). *Earth and Planetary Science Letters*, 289(1-2), 189–197. <http://doi.org/10.1016/j.epsl.2009.11.008>
- SSNERR. (2016). Retrieved from <http://www.oregon.gov/dsl/SSNERR/Pages/researchmonitoring.aspx> on May 10, 2016.

- Tribovillard, Nicolas, Thomas J. Algeo, Timothy Lyons, and Armelle Riboulleau. 2006. "Trace Metals as Paleoredox and Paleoproductivity Proxies: An Update." *Chemical Geology* 232 (1-2) (August): 12–32. doi:10.1016/j.chemgeo.2006.02.012. <http://linkinghub.elsevier.com/retrieve/pii/S000925410600132X>.
- USACE. (2015). Environmental Assessment, Coos Bay Maintenance Dredging, Coos County, Oregon.
- USDA. (2016). Census of Agriculture Historical Archive. Retrieved from <http://agcensus.mannlib.cornell.edu/AgCensus/homepage.do> on September 11, 2016.
- Wallick, J. R., O'Connor, J. E., Anderson, S., Keith, M., Cannon, C., & Risley, J. C. (2011). *Channel Change and Bed-Material Transport in the Umpqua River Basin, Oregon*. Reston, Virginia.
- Weltje, G. J., & Tjallingii, R. (2008). Calibration of XRF core scanners for quantitative geochemical logging of sediment cores: Theory and application. *Earth and Planetary Science Letters*, 274(3-4), 423–438. <http://doi.org/10.1016/j.epsl.2008.07.054>
- Wilson, C. G., Matisoff, G., & Whiting, P. J. (2007). The Use of <sup>7</sup>Be and Pb xs to Differentiate Fine Suspended Sediment Sources in South Slough, Oregon. *Estuaries and Coasts*, 30(2), 348–358.
- Yang, Y., Zhang, S., Yang, J., Chang, L., Bu, K., & Xing, X. (2014). A review of historical reconstruction methods of land use/land cover. *Journal of Geographical Sciences*, 24(4), 746–766. <http://doi.org/10.1007/s11442-014-1117-z>
- Youst, Lionel. (1997). *She's Tricky like Coyote Annie Miner Peterson, an Oregon Coast Indian Woman*. Norman: University of Oklahoma Press.
- Zwolsman, J. J. G., Berger, G. W., & Van Eck, G. T. M. (1993). Sediment accumulation rates, historical input, postdepositional mobility and retention of major elements and trace metals in salt marsh sediments of the Scheldt estuary, SW Netherlands. *Marine Chemistry*, 44, 73–94. [https://doi.org/10.1016/0304-4203\(93\)90007-B](https://doi.org/10.1016/0304-4203(93)90007-B)
- Zhang, Y., Wallace, J. M., & Battisti, D. S. (1997). ENSO-like interdecadal variability: 1900-93. *Journal of Climate*, 10(5), 1004–1020. [http://doi.org/10.1175/1520-0442\(1997\)010<1004:ELIV>2.0.CO;2](http://doi.org/10.1175/1520-0442(1997)010<1004:ELIV>2.0.CO;2)
- Zheng, Y., Anderson, R. F., Van Geen, A., & Kuwabara, J. (2000). Authigenic molybdenum formation in marine sediments: A link to pore water sulfide in the Santa Barbara Basin. *Geochimica et Cosmochimica Acta*, 64(24), 4165–4178. [http://doi.org/10.1016/S0016-7037\(00\)00495-6](http://doi.org/10.1016/S0016-7037(00)00495-6)